AFRL-ML-WP-TP-2007-494

PLATINUM ACETYLIDE TWO-PHOTON CHROMOPHORES (PREPRINT)

Aaron R. Burke and Thomas M. Cooper

Hardened Materials Branch
Survivability and Sensor Materials Division

APRIL 2007

Approved for public release; distribution unlimited.

See additional restrictions described on inside pages

STINFO COPY

AIR FORCE RESEARCH LABORATORY
MATERIALS AND MANUFACTURING DIRECTORATE
WRIGHT-PATTERSON AIR FORCE BASE, OH 45433-7750
AIR FORCE MATERIEL COMMAND
UNITED STATES AIR FORCE

NOTICE AND SIGNATURE PAGE

Using Government drawings, specifications, or other data included in this document for any purpose other than Government procurement does not in any way obligate the U.S. Government. The fact that the Government formulated or supplied the drawings, specifications, or other data does not license the holder or any other person or corporation; or convey any rights or permission to manufacture, use, or sell any patented invention that may relate to them.

This report was cleared for public release by the Air Force Research Laboratory Wright Site (AFRL/WS) Public Affairs Office and is available to the general public, including foreign nationals. Copies may be obtained from the Defense Technical Information Center (DTIC) (http://www.dtic.mil).

AFRL-ML-WP-TP-2007-494 HAS BEEN REVIEWED AND IS APPROVED FOR PUBLICATION IN ACCORDANCE WITH ASSIGNED DISTRIBUTION STATEMENT.

*//Signature//

THOMAS M. COOPER, Ph.D.
Agile Limiters Project
Exploratory Development
Hardened Materials Branch

//Signature//

MARK S. FORTE, Acting Chief
Hardened Materials Branch
Survivability and Sensor Materials Division

//Signature//

TIM J. SCHUMACHER, Chief
Survivability and Sensor Materials Division

This report is published in the interest of scientific and technical information exchange, and its publication does not constitute the Government's approval or disapproval of its ideas or findings.

*Disseminated copies will show "//Signature//" stamped or typed above the signature blocks.

REPORT DOCUMENTATION PAGE

Form Approved
OMB No. 0704-0188

The public reporting burden for this collection of information is estimated to average 1 hour per response, including the time for reviewing instructions, searching existing data sources, searching existing data sources, gathering and maintaining the data needed, and completing and reviewing the collection of information. Send comments regarding this burden estimate or any other aspect of this collection of information, including suggestions for reducing this burden, to Department of Defense, Washington Headquarters Services, Directorate for Information Operations and Reports (0704-0188), 1215 Jefferson Davis Highway, Suite 1204, Arlington, VA 22202-4302. Respondents should be aware that notwithstanding any other provision of law, no person shall be subject to any penalty for failing to comply with a collection of information if it does not display a currently valid OMB control number. **PLEASE DO NOT RETURN YOUR FORM TO THE ABOVE ADDRESS**.

1. REPORT DATE *(DD-MM-YY)*	2. REPORT TYPE	3. DATES COVERED *(From - To)*
April 2007	Journal Article Preprint	

4. TITLE AND SUBTITLE
PLATINUM ACETYLIDE TWO-PHOTON CHROMOPHORES (PREPRINT)

5a. CONTRACT NUMBER
In-house

5b. GRANT NUMBER

5c. PROGRAM ELEMENT NUMBER
62102F

6. AUTHOR(S)
Joy E. Rogers (UES)
Jonathan E. Slagle (AT&T Government Solutions)
Douglas M. Krein (General Dynamics Information Technology, Inc.)
Aaron R. Burke and Thomas M. Cooper (AFRL/MLPJ)
Benjamin C. Hall (Universal Technology Corporation)
Albert Fratini (University of Dayton)
Daniel G. McLean (Science Applications International Corporation)

5d. PROJECT NUMBER
4348

5e. TASK NUMBER
RG

5f. WORK UNIT NUMBER
M08R1000

7. PERFORMING ORGANIZATION NAME(S) AND ADDRESS(ES)

UES
4401 Dayton-Xenia Road
Dayton, OH 45432

AT&T Government Solutions
Dayton, OH 45324

General Dynamics Information Technology, Inc.
Dayton, OH 45431

Hardened Materials Branch (AFRL/MLPJ)
Survivability and Sensor Materials Division
Materials and Manufacturing Directorate
Wright-Patterson Air Force Base, OH 45433-7750
Air Force Materiel Command, United States Air Force

Universal Technology Corporation
Dayton, OH 45432

University of Dayton
Department of Chemistry
Dayton, OH 46469

Science Applications International Corporation
Dayton, OH 45433

8. PERFORMING ORGANIZATION REPORT NUMBER
AFRL-ML-WP-TP-2007-494

9. SPONSORING/MONITORING AGENCY NAME(S) AND ADDRESS(ES)
Air Force Research Laboratory
Materials and Manufacturing Directorate
Wright-Patterson Air Force Base, OH 45433-7750
Air Force Materiel Command, United States Air Force

10. SPONSORING/MONITORING AGENCY ACRONYM(S)
AFRL/MLPJ

11. SPONSORING/MONITORING AGENCY REPORT NUMBER(S)
AFRL-ML-WP-TP-2007-494

12. DISTRIBUTION/AVAILABILITY STATEMENT
Approved for public release; distribution unlimited.

13. SUPPLEMENTARY NOTES
Journal article submitted to Chemistry of Materials. The U.S. Government is joint author of this work and has the right to use, modify, reproduce, release, perform, display, or disclose the work. PAO Case Number: AFRL/WS 07-0647, 21 Mar 2007.

14. ABSTRACT
To explore the photophysics of platinum acetylide chromopores having strong two photon cross section, we have investigated the synthesis and spectroscopic characterization of a series of platinum acetylide complexes that feature highly π-conjugated ligands substituted with π-donor or –acceptor moieties. The molecules (numbered 1-4) considered in the present work are NLO-functionalized analogs of bis(phenylethynyl)bis(bributylphosphine)platinum(II) complexes. Molecule 1 carries two benzothiazolylfluorene and molecule

Continued on reverse side

15. SUBJECT TERMS Platinum Acetylide Chromopores, Fluorenyl ligand, oligomer

16. SECURITY CLASSIFICATION OF:			17. LIMITATION OF ABSTRACT:	18. NUMBER OF PAGES	19a. NAME OF RESPONSIBLE PERSON (Monitor)
a. REPORT	b. ABSTRACT	c. THIS PAGE			Thomas M. Cooper
Unclassified	Unclassified	Unclassified	SAR	64	19b. TELEPHONE NUMBER *(Include Area Code)* N/A

Standard Form 298 (Rev. 8-98)
Prescribed by ANSI Std. Z39-18

14. ABSTRACT

2 carries two diphenylaminofluorene substituents bound to the central platinum atom. Compounds 3 and 4 possess two dihexylaminophenyl substituents at their ends and differ by the number of platinum atoms in the oligomer "core" (one *vs*. two in 3 and 4, respectively). The conjugated ligands impart the complexes with effective two-photon absorption cross sections, while the heavy metal platinum centers give rise to efficient intersystem crossing to afford long lived triplet states. Photophysical studies demonstrate that one-photon excitation of the chromophores produces and S1 state that is delocalized across the two conjugated liglands, with weak (excitonic) coupling through the platinum center(s). The S_1 state is observed by ultrafast transient absorption and by its characteristic fluorescence. Intersystem crossing occurs rapidly ($k_{isc} \approx 1011\ s^{-1}$) to produce the T_1 state, which is believed to be localized on a single conjugated fluorenyl ligand. The triplet state is strongly absorbing ($\varepsilon_{TT} > 5 \times 10^4\ M^{-1}cm^{-1}$) and it is very long-lived ($\tau > 100\ \mu s$). Femtosecond pulses were used to characterize the two-photon absorption properties of the complexes, and all of the chromophores are relatively efficient two photon absorbers in the visible and near-infrared region of the spectrum (600 – 800 nm). The complexes exhibit maximum two-photon absorption at a shorter wavelength than 2λ for the one-photon band, consistent with the dominant two photon transition arising from a two-photon allowed gerade-gerade transition. Nanosecond transient absorption experiments carried out on several of the complexes with excitation at 803 nm confirm that the long-lived triplet state can be produced efficiently via a sequence involving two-photon excitation to produce S_1 followed by intersystem cross to afford T_1.

Platinum Acetylide Two-Photon Chromophores

[1,2]Joy E. Rogers, [1,3]Jonathan E. Slagle, [1,4]Douglas M. Krein, [1]Aaron R. Burke, [1,5]Benjamin C. Hall,

*[1,6]Albert Fratini, [1,7]Daniel G. McLean and [1]Thomas M. Cooper**

[1]Materials and Manufacturing Directorate, Air Force Research Laboratory, Wright-Patterson Air Force Base, OH 45433

[2]UES, Inc., Dayton, OH 45432

[3] AT&T Government Solutions, Dayton, OH 45324

[4]General Dynamics Information Technology, Dayton, OH 45431

[5]Universal Technology Corporation, Dayton, OH 45432

[6]Department of Chemistry, University of Dayton, Dayton, OH 45469

[7]Science Applications International Corporation, Dayton, OH 45431

*[8]Mikhail Drobizhev, [8]Nikolay S. Makarov and [8]Aleksander Rebane**

[8]Physics Department, Montana State University, Bozeman, MT 59717

*[9]Kye-Young Kim, [9]Richard Farley and [9]Kirk S. Schanze**

[9]Department of Chemistry, University of Florida, Gainesville, FL 32611

Abstract

To explore the photophysics of platinum acetylide chromophores having strong two photon cross section, we have investigated the synthesis and spectroscopic characterization of a series of platinum acetylide complexes that feature highly π-conjugated ligands substituted with π-donor or –acceptor moieties. The molecules(numbered **1-4**) considered in the present work are NLO-functionalized analogs of bis(phenylethynyl)bis(tributylphosphine)platinum(II) complexes. Molecule **1** carries two benzothiazolylfluorene and molecule **2** carries two diphenylaminofluorene substituents bound to the central platinum atom. Compounds **3** and **4** possess two dihexylaminophenyl substituents at their ends and differ by the number of platinum atoms in the oligomer "core" (one *vs.* two in **3** and **4**, respectively). The conjugated ligands impart the complexes with effective two-photon absorption cross sections, while the heavy metal platinum centers give rise to efficient intersystem crossing to afford long lived triplet states. Photophysical studies demonstrate that one-photon excitation of the chromophores produces an S_1 state that is delocalized across the two conjugated ligands, with weak (excitonic) coupling through the platinum center(s). The S_1 state is observed by ultrafast transient absorption and by its characteristic fluorescence. Intersystem crossing occurs rapidly ($k_{isc} \approx 10^{11}$ s^{-1}) to produce the T_1 state, which is believed to be localized on a single conjugated fluorenyl ligand. The triplet state is strongly absorbing ($\varepsilon_{TT} > 5 \times 10^4$ $M^{-1}cm^{-1}$) and it is very long-lived ($\tau > 100$ μs). Femtosecond pulses were used to characterize the two-photon absorption properties of the complexes, and all of the chromophores are relatively efficient two photon absorbers in the visible and near-infrared region of the spectrum (600 – 800 nm). The complexes exhibit maximum two-photon absorption at a shorter wavelength than 2λ for the one-photon band, consistent with the dominant two photon transition arising from a two-photon allowed gerade-gerade transition. Nanosecond transient absorption experiments carried out on several of the complexes with excitation at 803 nm confirm that the long-lived triplet state can be produced efficiently via a sequence involving two-photon excitation to produce S_1 followed by intersystem crossing to afford T_1.

Introduction

Interest in two-photon absorbing materials has increased within the past decade due to their usefulness in various applications. Specifically they are being developed for use in optical data storage[1, 2], frequency upconverted lasing,[3-5] nonlinear photonics,[6-8] microfabrication,[9,10] fluorescence imaging,[11] and photodynamic therapy.[12] Instantaneous absorption of two lower energy photons results in initiation of the same photophysical processes as one-photon absorption (1PA) of one high-energy photon. This is advantageous for two reasons. The first is that because of the use of a lower energy photon a material will be guarded from ionization effects from multiphoton absorption in the higher energy range that lead to its photodegradation. Secondly, because there is a quadratic dependence of two-photon absorption (2PA) on the intensity, the absorption only takes place in a small region of the focus allowing for more control in certain applications.

Over the years much research has gone into developing two-photon absorbing materials and trying to understand what controls their 2PA properties. A generally accepted method is to develop chromophores with large changes in polarization upon excitation.[13] This is achieved through either D-π-A (donor group-π-conjugated group-acceptor group), D-π-D, or A-π-A structural motifs and many such materials have been designed, showing remarkable increases in 2PA cross-sections.[14-23] For many two-photon absorbing molecules there is invariably a considerable discrepancy in the "effective" 2PA cross-section obtained by using differing pulse widths. A dramatic enhancement of this value in the nanosecond compared to femtosecond regime has been observed repeatedly in many cases.[24] This enhanced loss in nonlinear transmission of nanosecond pulses was attributed to contributions from the excited state absorption.[8, 25] Recently we were able to experimentally confirm that this effect is indeed due to absorption from both the singlet and triplet excited states.[26, 27] Therefore to enhance the nanosecond nonlinear absorption we are interested in developing materials with large excited state absorption.

Here we describe materials with large triplet excited state population following laser excitation. To ensure a large triplet population we have added platinum to the center of the molecule. Shown in Figure 1 are the structures of **1**, **2**, **3**, and **4**. Their overall structure is based on a series of platinum poly-ynes that we and others had previously studied but with the exception of new types of ligands.[28-32] The ligands consist of a central π-conjugated fluorenyl group attached to either an electron donating amino-fluorenyl or electron withdrawing benzothiazolyl-fluorene that are themselves known as two-photon absorbing dyes.[19, 20, 33-39] These materials have a donor-π-donor (**2**, **3**, and **4**) or acceptor-π-acceptor (**1**) motif. We wanted to draw on our experience of working with the platinum poly-ynes and two-photon materials to create new molecules that give strong 2PA in the red and near-IR part of spectrum. An insertion of platinum is needed to promote high intersystem crossing yields.

In the literature there are several examples of Pt chromophores that exhibit 2PA in the visible and near-IR region. Bis((4-phenylethynyl)phenyl)ethynyl)bis(tributylphosphine)platinum(II) (**PE2**) has a measurable intrinsic (femtosecond) 2PA cross section (σ_2) of 7 GM at 720 nm.[32,40,41] The 2PA coefficient (β) of this molecule was first reported at 595 nm to be 0.34 cm/GW, which corresponds to 235 GM for σ_2.[28,42] The latter measurement was made using picosecond pulses, which allows for considerable excited state absorption from both the S_1 as well as the T_1 excited states. This would correctly be termed an effective two photon absorption cross-section. More recently, a dendron-decorated **PE2** series has been studied and shown to have similar to **PE2** intrinsic σ_2 values at 720 nm.[43] Also Pt poly-ynes substituted with thiophene groups in place of phenyl groups have shown a doubling of the intrinsic σ_2 value at 740 nm.[40, 41] In this paper we describe novel platinum dyes that contain either electron-accepting benzothiazolyl groups or electron-donating amino groups coupled through a central fluorene unit that do show a remarkable increase in the 2PA cross section (σ_2) over **PE2** mentioned above. We present the photophysical properties of these materials and discuss their structure - property relationships in terms of both 1PA and 2PA properties.

Experimental

Synthesis. Details on the synthesis of these materials are given in the supporting information.

General Techniques. Ground state UV/Vis absorption spectra were measured in 1 cm quartz cuvettes on either a Cary 100 (UF) or a Cary 500 (AFRL) spectrophotometer. Corrected steady state emission spectra were measured using either a Perkin Elmer model LS 50B fluorometer (AFRL) or a SPEX F-112 fluorometer (UF). Samples were contained in 1 cm quartz cuvettes, and the optical density was adjusted to approximately 0.1 at the excitation wavelength. Time correlated single photon counting (Edinburgh Instruments OB 920 Spectrometer) was utilized to determine singlet state lifetimes. The samples were pumped using either a 70-picosecond laser diode at 401 nm or a 70-picosecond laser diode at 375 nm. Emission was detected on a cooled microchannel plate PMT. Data was analyzed using a reconvolution software package provided by Edinburgh Instruments. Nanosecond time-resolved absorption spectra at the University of Florida were obtained on an instrument that has been previously described that uses the third harmonic of a Nd:YAG laser (Spectra Physics GCR-14, 355 nm, 10 ns fwhm, 10 mJ pulse^{-1}, 20 mJ·cm^{-2} irradiance) as excitation source.[44] Samples were deoxygenated by bubbling with nitrogen. Nanosecond transient absorption measurements at AFRL were carried out using the third harmonic (355-nm) of a Q-switched Nd:YAG laser (Quantel Brilliant, pulse width ca. 5 ns). Pulse fluences of up to 4 mJ cm^{-2} at the excitation wavelength were typically used. A detailed description of the laser flash photolysis apparatus has been published earlier.[29] All samples were deoxygenated by three successive freeze-pump-thaw cycles. Two-photon pumped transient absorption (AFRL) utilized the same laser flash photolysis apparatus but samples were pumped with the idler beam (803 nm) of a 355 nm optical parametric oscillator (OPO). Color filters removed the signal beam and residual 355nm and were verified. The idler beam was focused into the sample transverse to the white light probe with an energy of 4 mJ at 803nm. Samples were made at concentrations of 0.02 M and degassed by three cycles of freeze-pump-thaw. The probe was masked at 1 mm by 1cm at the front and rear face of the cuvette and imaged onto a 625 μm slit of a monochromator. The probe image could then be translated across the slit to a point just off the focus of the laser producing a transient spectrum.

Ultrafast transient absorption measurements were performed using a modified version of the femtosecond pump-probe UV-VIS spectrometer described elsewhere.[45] Briefly, 1mJ, 100 fs pulses at 800 nm at 1 kHz repetition rate were obtained from a diode-pumped, Ti:Sapphire regenerative amplifier (Spectra Physics Hurricane). The output laser beam was split into pump and probe (85 and 15%) by a beam splitter. The pump beam was directed into a frequency doubler (400 nm) (CSK Super Tripler) and then was focused into the sample. The probe beam was delayed in a computer-controlled optical delay (Newport MM4000 250 mm linear positioning stage) and then focused into a sapphire plate to generate white light continuum. The white light was then overlapped with the pump beam in a 2 mm quartz cuvette and then coupled into a CCD detector (Ocean Optics S2000 UV-VIS). Data acquisition was controlled by software developed by Ultrafast Systems LLC.

Fluorescence quantum yields were determined using the actinometry method previously described.[29] For **1**, **2**, **1-L**, and **2-L** quinine sulfate was used as an actinometer with a known fluorescence quantum yield of 0.55 in 1.0 N H_2SO_4.[46] These samples were excited at 330 nm (**1-L** and **2-L**) or 370 nm (**1** and **2**) with a matched optical density of 0.1. Fluorescence quantum yield for **3-L** was measured relative to Coumarin 30 in CH_3CN where $\phi = 0.67$.[47] Emission quantum yields for **3** and **4** are reported relative to $Ru(bpy)_3$ in air saturated water for which $\phi = 0.0379$ and an appropriate correction was applied for the difference in refractive indices of actinometer and sample solvent.[48] The triplet molar absorption coefficients of the four Pt compounds were determined using relative actinometry. Benzophenone was utilized as the actinometer with a known molar absorption coefficient of $\Delta\varepsilon_{525nm} = 7870 \pm 1200\ M^{-1}\ cm^{-1}$ and triplet quantum yield of $\Phi_T = 1.0$.[49, 50] Matched optical densities of 0.8 of **1**, **2**, **3**, **4**, and benzophenone at 355 nm were utilized in each determination. While the O.D. is higher than normally used with a right angle geometry, inner filter effects were avoided by the geometry for the collection of the probe beam light. Data were obtained at various laser fluence ranges to pinpoint useful ranges in the data where nonlinear effects are not occurring. The linear working range was usually 0 – 500 $\mu J/cm^2$ for Pt complexes and up to ~ 4 mJ/cm^2 for benzophenone. ΔA at each energy was determined and then

plotted as a function of laser fluence for both the unknown samples and the benzophenone. The following expression (equation 1) was used to obtain $\Delta\varepsilon_{sam}$ of the sample.

$$\Delta\varepsilon_{sam} = \frac{slope_{sam}\phi_{ISCref}\Delta\varepsilon_{ref}}{slope_{ref}\phi_{ISCsam}} \quad (1)$$

Where $slope_{sam}$ and $slope_{ref}$ are the respective slopes, Φ_{ISCref} and Φ_{ISCsam} are the known intersystem crossing quantum yields of both the reference and the sample, and $\Delta\varepsilon_{ref}$ is the known molar absorption coefficient of the benzophenone.

Quantum yields for intersystem crossing were determined using the method of photoacoustic calorimetry (PAC). Details on PAC methods and instrumentations have been previously described.[51] Ferrocene was used as a calorimetric reference sample. Ferrocene releases heat in unity after excitation. All samples were degassed with nitrogen for 15 min and the measurements were taken under a nitrogen atmosphere. The data were taken at various laser fluences to minimize the nonlinear absorption effects. The linear laser power range was 0-30 μJ/pulse and the beam was focused through a 2.0 mm slit. The pressure wave produced after laser excitation was detected through a piezoelectric transducer with 1MHz bandwidth. Amplitude of each wave is plotted vs. laser energy. The ratio of the slopes represents ϕ_p. ISC quantum yields (Φ_{ISC}) were obtained from the following equation (2).

$$(\phi_p)\,(E_{h\nu}) = (E_{h\nu} - E_S) + (1 - \Phi_{ISC} - \Phi_F)\,E_S + \Phi_{ISC}\,(E_S - E_T) \quad (2)$$

Where ϕ_p is the fraction of the heat produced by the sample relative to the heat evolved by the reference solution, $E_{h\nu}$ is the energy that corresponds to excitation wavelength (355 nm = 80.5 kcal), E_S is the energy of singlet excited state of the sample and E_T is the energy of triplet excited state of the sample. Non-radiative decay of T_1 to S_0 is not considered in this calculation because PAC can not measure heat release on longer time scales such as tens of microseconds (triplet state) due to the 1 MHz frequency band limitations of transducer. As a control experiment, ϕ_{ISC} of benzophenone and anthracene were measured using ferrocene as an actinometer. ϕ_{ISC} of benzophenone and anthracene is

0.96 and 0.78, respectively. These numbers are within ±10% range compared to the previously reported value; $\phi_{ISC} = 1$ for benzophenone[50, 52] and $\phi_{ISC} = 0.71$ for anthracene.[53]

The laser system for two-photon absorption measurements comprised a Ti: sapphire femtosecond oscillator (Coherent Mira 900) pumped by 5W CW frequency-doubled Nd:YAG laser (Coherent Verdi) and a 1-kHz repetition rate Ti:sapphire femtosecond regenerative amplifier (Clark MXR CPA-1000). The pulses from the amplifier were down converted with an optical parametric amplifier, OPA (Quantronix TOPAS), whose output can be continuously tuned from 1100 to 2200 nm. The second harmonic of signal and idler was used for two-photon excitation in λ_{ex} = 550 – 800 nm and λ_{ex} = 800 – 1100 nm regions, respectively. The OPA output signal pulse energy was 100 - 200 μJ (20-30 μJ after frequency doubling of signal and 5 - 10 μJ after frequency doubling of idler), and pulse duration was 100 fs.

The linearly polarized excitation laser beam was slightly focused with an f = 25-cm cylindrical lens onto the sample solution contained in 1-cm spectroscopic cell and placed 15 cm behind the lens. A small fraction of the beam was split off by a thin glass plate placed just before the sample and directed to the reference detector (Molectron). The sample fluorescence was collected in frontal geometry with a spherical mirror (f = 50 cm, diameter d = 10 cm) and focused with magnification ratio ~ 1 on the entrance slit of an imaging grating spectrometer (Jobin Yvon Triax 550). The 2PA spectrum (in relative units) was obtained by tuning the wavelength of OPA, and measuring the corresponding intensity of two-photon excited fluorescence. The wavelength tuning of OPA and data collection were computer-controlled with a LabView routine. At each wavelength, the fluorescence intensity was normalized to the square of the excitation photon flux, measured in the reference channel. To exclude possible artifacts, e.g. due to absorption at wavelengths close to the linear absorption, we checked that at each wavelength the fluorescence signal increased as a square of the excitation intensity.

Absolute 2PA cross sections were measured using relative fluorescence technique at 650 nm excitation.[54] We used bis-diphenylamino stilbene solution in methylenechloride, for which σ_2 = 250

GM at 650 nm, as a standard.[55] To obtain absolute 2PA spectra in GM units, all relative 2PA spectra were calibrated to the known (at 650 nm) absolute cross section value.

Results

The design of new two-photon absorbing chromophores coupled with Pt complexes to produce large intersystem crossing to the triplet state and long-lived excited states has proven successful in this study. Shown in Figure 1 are the structures of the four Pt complexes **1**, **2**, **3**, and **4**. The first two complexes were synthesized at AFRL based on our previous work with a series of 2PA dyes. The design is based on the well known donor-π-conjugated-donor or the acceptor-π-conjugated-acceptor motifs, yielding materials that have significant near-IR 2PA strength. Chromophores **3** and **4** were synthesized at University of Florida and are based on the same donor-π-conjugated-donor concept but include additional acetylene/phenyl linkages as well as an additional Pt in chromophore **4**. Also shown in Figure 1 are the ligands of chromophores **1** – **4**. The latter molecules are included for comparison to the platinum containing chromophores. Details on the synthesis of all these materials are given in the supporting information. X-ray crystallography was accomplished for **1** and **2**. Details of these findings are also given in the supporting information. A notable structure result for compound **2** is that the angle between the fluorenyl carbon-nitrogen-phenyl carbon atoms is ~120 deg, showing the lone pair of electrons on the nitrogen has sp^2 hybridization, resulting in conjugation with the fluorenyl group. The bond length of the acetylene bonded to the platinum atom is 1.208 Å in compound **1**, but it is 1.144 Å in compound **2**.

Ground-State Absorbance. Quantified ground state absorption data for chromophores **1**, **2**, **3**, and **4** is given in panels a, b, and c of Figure 2. For comparison the ligands spectra of **1**, **2**, **3**, and **4** were recorded and presented in the corresponding panels in Figure 2. The singlet state energy of the ligands follows the trend E_S(**3-L**) < E_S(**2-L**) < E_S(**1-L**), while that of the platinum complexes follows the trend E_S(**1**) < E_S(**3**) ~ E_S(**4**) < E_S(**2**). Ligand **3-L** has red-shifted absorption relative to the other ligands. Wavelength maxima and molar extinction coefficients are given in Tables 1 and 2. Compared to their

corresponding ligands, **1**, **3**, and **4** all demonstrate a significant red shift of absorption spectrum, peaking at 395 – 400 nm, while compound **2** shows only slight shift, with a maximum at 380 nm. The magnitude of the red shift upon conversion of ligand to platinum complex follows the trend $|\Delta E_S(\mathbf{1})| > |\Delta E_S(\mathbf{2},\mathbf{3},\mathbf{4})|$. This is due to the increased conjugation through the acetylene-phenyl group. Chromophore **1** experiences quite a large red shift in its spectrum compared to the ligand **1-L**. Therefore, there is a large amount of conjugation in the ground state absorption of this chromophore compared to closely related chromophore **2**. The addition of the diphenylamino groups in place of the benzothiazolyl groups results in less conjugation and therefore **2-L** has a nearly identical absorption spectrum to **2**. For chromophores **3** and **4,** the absorption spectra are very similar with the main change only in the intensity. This indicates that the addition of the extra platinum atom and central phenyl ring does not contribute much to the ground state absorption.

Emission. Also shown in Figure 2, panels d, e, and f, are the emission spectra of all the chromophores in benzene. For the Pt complexes both the fluorescence (350 – 550 nm range) and room-temperature phosphorescence (550 – 750 nm range) under deoxygenated conditions are observed. The data have been normalized for comparison. Room temperature phosphorescence was not observed from the ligands, as would be expected. Fluorescence and phosphorescence quantum yields are given in Table 1. The ligands all have high fluorescence quantum yields which decrease by a factor of approximately 30 upon formation of the platinum complex. Comparing the fluorescence of the ligands to that of the Pt complexes, it is interesting to note that the spectra of **2** and **2-L** are identical and the spectra of **3**, **4**, and **3-L** are also similar. This is not the case for **1** and **1-L**. The spectra are quite different in shape and the fluorescence from complex **1** is red-shifted compared to ligand **1-L**. The phosphorescence of **2** is blue-shifted compared to **1**, **3**, and **4**. Interestingly, the phosphorescence of the latter three overlap almost exactly, indicating that the triplet energies in these three complexes are the same Time correlated single photon counting (TCSPC) was utilized to measure the singlet state lifetimes. For all of the platinum complexes the emission decays well within the instrument response function of less than 50 ps, not providing useful information.

Transient Absorption. The femtosecond pump-probe technique was utilized to measure the S_1-S_n transient absorption spectrum of each compound and also to study the fast dynamics of relaxation. These data are shown in Figure 3 for **1**, **2**, and **3**. We also obtained time resolved spectra for **4** but have not included them since they are nearly identical to those of **3**. Shown are transient spectra, obtained at various time delays ranging from immediately following the laser pulse to 48 ps after the pulse. For each chromophore we observe biexponential decay kinetics. The faster decay involves a slight spectral shift as evidenced in Figure 3. The lifetimes of the faster decay are 6.7 ± 0.5 ps (**1**), 4.8 ± 0.2 ps (**2**), 2.5 ± 0.3 ps (**3**), and 4.2 ± 0.2 ps (**4**). We attribute this to internal conversion from higher singlet states and vibrational relaxation as well as solvent reorganization about the molecule. The slower decay is assigned to intersystem crossing of the relaxed singlet state to the triplet state. The intersystem crossing lifetimes for this process are given in Table 2. A large shift in the transient spectrum associated with intersystem crossing, is evidenced in Figure 3 for all materials. Compounds **1**, **3** and **4** show a 25 nm red shift. Compound **2** has anomalous behavior, with the initial excited-state absorption spectrum showing a 25 nm blue shift upon relaxation and also an additional peak at 525 nm that disappears with time. In all cases there is an isobestic point, indicating the interconversion between two species. The transient absorption spectrum appearing 48 ps after the 100 fs excitation is identical with that obtained in nanosecond laser flash photolysis experiments (described below), which confirms its assignment to triplet-triplet absorption. A further evidence that intersystem crossing takes place on a timescale < 50 ps can be found in time-correlated single-photon counting data. The singlet lifetimes obtained with this method were less than 50 ps (i.e. within instrument response) for all materials in air saturated benzene, which is consistent with the ultrafast transient absorption data. The triplet state is rapidly formed, then decays only slightly within the time scale limit of the ultrafast transient absorption (1.6 ns). The triplet lifetimes obtained with nanosecond laser flash photolysis under both air-saturated and deoxygenated conditions are presented in Table 2.

Nanosecond transient absorption spectra are shown in Figure 4. The data have been quantified using the method of relative actinometry. Chromophores **1**, **3**, and **4** have maximum peaks at 670 nm,

while **2** is blue-shifted with a peak at 610 nm. Also it is interesting to note that the maximum molar absorption coefficient of **2** is less than one-half of the other chromophores. These values are given in Table 2. The triplet excited state was confirmed via oxygen quenching. The triplet lifetimes under both air saturated and deoxygenated conditions are also presented in Table 2. Intersystem crossing quantum yields were measured using photoacoustic calorimetry (PAC) and are collected in Table 2. All compounds give strong intersystem crossing with quantum efficiency near unity, consistent with the short singlet lifetimes

Two-photon absorption. Two-photon absorption (2PA) spectra are presented in Fig. 5. In general, all four compounds show a similar behavior. One may distinguish three distinct spectral regions – short-, middle- and long-wavelengths. In the long-wavelength region, $\lambda_{ex} > 850$ nm, 2PA gradually decreases towards long wavelengths. The middle region is that around the one-photon absorption peak, and one observes a moderately strong 2PA transition. The 2PA maximum almost coincides with the corresponding 1PA peak at $\lambda_{ex} \approx 2\lambda_{1PA}$. In the short-wavelength region, $\lambda_{ex} = 600 - 700$ nm, a strong isolated 2PA peak shows up in all cases.

For quantitative comparison of 2PA strength of our functionalized molecules with **PE2** and other analogs, it is more reasonable to consider an integrated 2PA strength of the short-wavelength peak, which can be defined as $F = \int\sigma_2\, d(2\nu)$, where ν is the laser frequency in cm^{-1}. These values, along with maximum 2PA cross sections and spectral widths of 2PA transition, Γ_f, are collected in Table 3. We note here, that according to definition, the 2PA cross section obtained with relative fluorescence technique σ_2' is twice of that obtained with nonlinear transmission methods (such as z-scan):[53] $\sigma_2' = 2\sigma_2$. Therefore, for the sake of comparison, Tables 3 and 4 present all the data in terms of σ_2. As one can see, both the maximum value and the integrated strength of 2PA transition is greater for all compounds **1** – **4**, compared to **PE2**.

Table 4 presents nonlinear absorption parameters, relevant for higher order multiphoton processes at a few selected wavelengths. The first two columns compare the effective 2PA cross sections at 595 and at

720 nm measured in this work for **1** - **4** and those obtained in the literature for **PE2**. As one can see, all the compounds studied here greatly outperform **PE2** at 720 nm and show σ_2 of the same order or larger than **PE2** at 595 nm (see more details in Discussion). The next three columns of the Table comprise the maximum triplet-triplet (T-T) transient absorption cross section (recalculated from data in Table 2), the width of the triplet-triplet absorption spectrum (Fig. 4), and the triplet lifetime (Table 2). As one can see from the Table 4, again all the molecules **1** – **4** possess a favorable set of parameters compared to **PE2**. Slightly lower σ_1^{T-T} value for **2**, compared to PE2, is greatly offset by a much larger σ_2 value, as well as a wider T-T absorption.

Two Photon Pumped Transient Absorption. A modified laser flash photolysis experiment was utilized to confirm the ability of these compounds to populate the triplet excited state via two-photon absorption. In this experiment all samples were prepared at 0.02 M and were excited with a 5 ns, 803 nm pump pulse. Details of the experiment are given in the experimental section. The spectra obtained for **3** and **4** are shown in Figure 6. They are identical to the spectra shown in Figure 4. These results prove that regardless of excitation mode (1PA or 2PA), ultimately formation of the triplet excited state is realized. Examples of lifetimes obtained under these conditions are significantly shorter than those collected under one-photon excitation conditions seen in Table 2, compound **3**: 3.5 *vs.* 213 μs, compound **4**: and 2.7 *vs.* 238 μs. We believe this to be due to a self-quenching mechanism, common in a similar Pt complex that is more noticeable at higher concentrations used in 2PA experiment.[56]

Discussion

Excited State Structure and One-Photon Photophysics. The molecules considered in the present work are NLO-functionalized analogs of bis(phenylethynyl)bis(tributylphosphine) platinum (II) (**PE1**) and bis((4-(phenylethynyl)phenyl)ethynyl)bis(tributylphosphine) platinum (II) (**PE2**). Molecule **1** carries two benzothiazolylfluorene and molecule **2** – two diphenylaminofluorene substituents instead of two phenyl substituents in **PE1**. Compounds **3** and **4** possess two dihexylaminophenyl substituents at their

ends and differ by the number of platinum atoms in the oligomer "core" (one vs two in **3** and **4**, respectively). The objective of this work is to characterize all of the photophysical processes of these materials as shown in the Jablonski diagram shown in Scheme 1. The chromophores were designed to undergo efficient two-photon excitation to the S_1 (or higher) state with red or near-IR photons and then from there to undergo various relaxation processes including intersystem crossing to the triplet excited state. In this work we show that for these materials the photophysical processes are the same, regardless of the mode of excitation (1PA or 2PA), as it would be expected according to Kasha's rule.

The ground state absorption spectra of platinum acetylide complexes have been shown to be dominated by the allowed transition between the HOMO and LUMO levels. To a first approximation, the transition is primarily intra-ligand $\pi\pi^*$; however, the transition does involve a small degree of metal-to-ligand (MLCT).[57,58] The HOMO of platinum acetylides typically consists of a small contribution from the (in-plane) d_{xy} orbital on the platinum center combined with π-symmetry orbitals on the ligands. The LUMO is centrosymmetric and is comprised exclusively of ligand-localized orbitals having π-symmetry (because of the centrosymmetry the MO has no contribution from $d\pi$ orbitals on the platinum atom). Given that the lowest optical transition is dominated by HOMO $\rightarrow$ LUMO and the highly delocalized nature of these orbitals it is evident that the S_1 state is delocalized through the central platinum atom (i.e., it is not localized on a single acetylide ligand). The notion that the Frank Condon singlet state is more delocalized in the complexes than in the free acetylene ligands is supported by the fact that the strongly allowed absorption is red-shifted in complexes compared to the ligands.

A previous study of the homologous series of platinum acetylides *trans*-$Pt((P(C_4H_9)_3)_2((C{\equiv}C\text{-}C_6H_4)_n\text{-}H)_2$, n = 1-3, and analogous set of butadiynes gives a relation between end-to-end chromophore length and the singlet energy, E_S.[59] Using that relation and the end-to-end lengths of compounds **1** - **3**, we estimated their E_S values, and in all three cases the relation overestimates the experimental E_S values by 0.1 – 0.2 eV. The largest difference (~0.2 eV) is in compound **1**. The difference between the previously studied chromophores and compounds **1** - **3** is the presence of the strongly conjugated units

in the acetylide ligands. In particular, it is likely the high electron affinity of the benzothiazolyl group in compound **1** introduces intraligand charge-transfer character and also induces delocalization of the S_1 state into the heteroaromatic ring system. The 4-(dialkylamino)phenylethynyl substituents on the fluorene ligand in **3** and **4** also provide increased π-conjugation in the S_1 state. By contrast, the excited state is comparatively more localized in **2**; although the amino substitutent is electron donating and may introduce some charge-transfer character, the excitation is localized primarily on the fluorene units, resulting in a relatively higher energy S_1 and T_1 state in this complex.

The strength of interaction between the central platinum atom and the ligand is deduced from the length of the ethynyl group attached to the central platinum atom. The longer bond length determined from the X-Ray structure in **1** compared to **2** is evidence for back bonding from the platinum atom to the ligand, resulting from the electron-withdrawing effect of the benzothiazole group. The lack of back bonding in **2** is supported by the shorter ethynyl bond length, resulting from the electron-donating effect of the diphenylamino group.

In previous work, we have demonstrated that in platinum acetylides the triplet exciton is relatively confined, and is localized on a single acetylide ligand, as opposed to being delocalized across the entire complex through the Pt center.[58] In keeping with this concept, we believe that in the series of complexes **1 – 4** the triplet exciton is confined to a single conjugated acetylide ligand. In particular, the triplet energies (T_1) of the complexes are reflected by the phosphorescence emission band maxima, which lie at ≈ 2.20 eV in **1**, **3** and **4** and at ≈ 2.32 eV in **2**. As a point of reference, the triplet energy of 9,9-dihexylfluorene is 2.86 eV and for an oligomer containing three 9,9-dihexylfluorene repeats is 2.25 eV.[60] This comparison indicates that the triplet exciton in all of the complexes is delocalized beyond the fluorene unit, likely extending into the ethynylene units as well as into the additional aromatic ring systems in **1**, **3** and **4**. Note that the phosphorescence spectra of **3** and **4** are superimposable, which underscores the fact that the triplet is localized in the more highly conjugated fluorenyl ligand system, rather than being localized in the [-Pt-C≡C-C_6H_4-C≡C-Pt-] chromophore, which is known to have a triplet energy of 2.40 eV.[30] Interestingly, the triplet energy in **2** is higher than in the other complexes,

and this is clearly due to the smaller conjugated system that is available in this complex's ligand system. Similar behavior is seen in the nanosecond transient absorption spectra, where compounds **1**, **3** and **4** have the same maximum, while **2** has a blue shift, suggesting a smaller conjugation length in **2**. From the intersystem crossing and phosphorescence quantum yields, the average radiative rate constant is $k_{ph} \sim 10^2\ s^{-1}$, while the average non-radiative intersystem crossing rate constant is $k_{isc}(T_1 \rightarrow S_0) \sim 10^4\ s^{-1}$. The non-radiative decay rate constant is similar to published results showing a relation between energy gap and decay rate.[61]

The femtosecond transient absorption spectra shown in Figure 3 provide a probe into the intersystem crossing process in the platinum acetylide chromophores. In all cases, initial excitation into the Franck-Condon S_1 excited state is followed by relaxation into the T_1 state within 48 ps after the 100 fs laser pulse. The short singlet state lifetime in the Pt-complexes is consistent with intersystem crossing being very rapid. This finding is in accord with expectation given the strong spin-orbit coupling which is induced by the heavy metal Pt atom. As described in a recent review of femtosecond absorption spectroscopy of transition metal complexes,[62] the processes occurring upon excitation include intersystem crossing, vibrational and solvent relaxation. In transition metal complexes, intersystem crossing can be very rapid due to strong spin-orbit coupling induced by mixing of the ligand (π and π^*) and metal ($d\pi$) orbitals. For example, the intersystem crossing time of $[Ru(bpy)_3]^{2+}$ is 40 fs,[63] while McCusker[62] describes solvent diffusion and vibrational relaxation occurring on a ps timescale. In the ultrafast transient absorption spectra of platinum acetylides **1 - 4**, spectroscopic changes are observed that are associated with initial excitation, vibrational cooling, solvent relaxation and conversion to the relaxed T_1 state. From the measured singlet state lifetimes and intersystem crossing quantum yields, the intersystem crossing rates range from $10^{10} - 10^{11}\ s^{-1}$, showing strong mixing of the S_1 and T_1 states. From the intersystem crossing and fluorescence quantum yields, the rates of fluorescence decay and internal conversion are comparable($k_{fl} \approx k_{ic} \sim 10^9\ s^{-1}$). This behavior contrasts with the d^6 metal complex systems (e.g., $Ru(bpy)_3^{2+}$), where the singlet-triplet mixing is considerably stronger, and it is

not possible to observe a distinct spectroscopic signature of a singlet state prior to intersystem crossing ($k_{isc} > 10^{12}$ s^{-1}).

An interesting point is that the ultrafast transient absorption spectra and dynamics observed for complex **2** are different compared to those of compounds **1**, **3** and **4**. In particular, the transient spectrum immediately after excitation features bands at 525 and 675 nm. On a timescale of approximately 10 ps the 525 nm peak decays and the band in the red part of the spectrum blue shifts to 640 nm, with conversion complete within 30 ps. A possible explanation for this behavior can be found in a recent study of the ultrafast transient absorption dynamics of a triphenylamine chromophore.[64] In this manuscript the authors report femtosecond transient absorption spectra of tris-4,4',4''-(4-nitrophenylethynyl)triphenylamine, which initially features bands at 500 nm and 650 nm followed by spectral evolution and dynamics which are quite similar to those observed for **2**. The authors conclude that the spectra arise due to relaxation of a Frank-Condon state that is completely delocalized through the C_3 symmetry triphenylamine chromophore, which undergoes rapid relaxation into a charge transfer state that is localized on a single conjugated unit (C_1 symmetry). In complex **2** a diphenylamino chromophore is attached to the fluorenyl group; thus, the ligand can be viewed as a fluorenyl substituted triphenylamine chromophore. It is possible that in the Franck-Condon state of this complex the excitation is delocalized on the triarylamine chromophore (pseudo-C_3 symmetry), and the relaxation that takes place on the ps timescale involves localization of the excitation into the fluorenyl-acetylide chromophore, followed by intersystem crossing to produce the triplet state. Evidence for the contribution of the triarylamine portion of the ligand to the Franck-Condon state can be found from the X-Ray diffraction results for **2**, where the carbon-nitrogen-phenyl bond angle being 120 deg results in conjugation between the phenyl groups and the rest of the chromophore.

Two-Photon Absorption and Photophysics. The two photon absorption properties of some linear platinum-organic compounds with various side ligands were previously studied theoretically by Norman et al.[57] According to calculations, both centrosymmetric and non-centrosymmetric structures have a broad set of 2PA allowed transitions in the visible part of the spectrum. One particularly strong

transition that occurs at an energy higher than the lowest 1PA transition dominates. Our data qualitatively reproduces this theoretical picture, especially if we consider that 2PA transition frequencies obtained from calculations are often higher than observed in experiment.[57] A significant fact is that the very strong 2PA peak experimentally observed in the region λ_{ex} = 600 – 700 nm (see Fig. 5) is universal for all four of the complexes and it is not reproduced in the one-photon absorption (there are no isolated peaks at 300 – 350 nm in 1PA). This 2PA peak can be tentatively assigned to a one-photon forbidden, but two-photon allowed gerade-gerade transition. This, in turn, implies that the absorbing species possess inversion symmetry and therefore the Pt atom is involved in the conjugated system. On the other hand, all compounds show also a much weaker, but distinct 2PA peak at λ_{ex} = 750 – 800 nm, which is nearly coincident with the 1PA maximum. There are two possible explanations to this apparent violation of the alternative selection rule. First, both bands may be observed due to a different coupling of the electronic transition to non-totally symmetric vibrations in 1PA and 2PA. The second possibility is that in the solution there are at least two different conformers, at least one of them being centrosymmetric, while the others are not. The first possibility (vibronic coupling) seems less probable, because the observed 2PA band is moderately-strong: σ_2' ~ 150 – 300 GM (1 GM = 10^{-50} cm^4 s) in **2** and **3** and even stronger ~ 900 GM in **1**. This should imply a non-realistically large change of permanent dipole moment (5 - 10 D) due to non-symmetrical vibration. Also, such a violation of selection rules has not been observed in other one-dimensional centrosymmetric oligo-phenylene-vinylene family of molecules.[24] In non-centrosymmetric conformers, the large change of permanent dipole moment can be imagined if, due to breaking of symmetry, a Franck-Condon excitation is localized on one ligand. Therefore, we tentatively assign the 2PA peak near 750 - 800 nm to the presence of non-centrosymmetric conformers.

It is interesting to note that 1PA spectra of centrosymmetric and non-centrosymmetric conformers were predicted to have coinciding transition frequencies and almost the same oscillator strengths (cf. compounds **mIIb** and **mIIc** in Table 3 of Norman[57]). If our assumption about different conformers is correct, then 2PA spectroscopy can be uniquely suited for distinguishing between these species. On the other hand, simultaneous presence of different types of conformers in the solution suggests that the 2PA

strength which are reported herein and are measured by the fluorescence technique, reflects perhaps not the true value but rather an effective weighted average of different conformers cross sections.

For simplicity suppose that there are two types of conformers – (centrosymmetric (conformer 1) and non-centrosymmetric (conformer 2). One can show then that if the two have an identical fluorescence spectrum, both in shape and in quantum efficiency (which, according to our preliminiary data seems to be the case for compounds studied here), then the measured effective 2PA cross section at each particular wavelength λ_{ex} is:

$$\sigma_2'^{(eff)}(\lambda_{ex}) = n_1 \sigma_2^{(1)}(\lambda_{ex}) + n_2 \sigma_2^{(2)}(\lambda_{ex}) \ , \qquad (3)$$

where indices 1 and 2 correspond to conformers 1 and 2 and n_i is equal to the mole fraction of the i-th conformer, such that $n_1 + n_2 = 1$. Without independent knowledge of n_i values, we cannot estimate separately $\sigma_2^{(1)}$ and $\sigma_2^{(2)}$. On the other hand, if our assignment of the 2PA peaks is correct, and since $n_i < 1$, each conformer will have an even larger maximum σ_2 value compared to that presented in Fig 5.

In the series of linear platinum acetylide multiphoton absorbers, **PE2** can be considered as a convenient benchmark, because it has been studied rather extensively.[28, 42, 43, 57, 65-71] Staromlynska and co-workers found the 2PA coefficient of **PE2** to be $\beta = 0.34$ cm/GW at 595 nm in 0.08 M solution.[28] This translates to 2PA cross section equal to 235 GM. Since this value was obtained with the z-scan technique and 27-ps pulses, the authors do not exclude an excited-state absorption contribution, and thus $\sigma_2 = 235$ GM can be considered as an upper limit for the intrinsic instantaneous 2PA cross section. This assumption finds further confirmation in the recent data of Vestberg et al., who obtained $\sigma_2 = 7$ GM in at 720 nm for **PE2** by using the z-scan technique and much shorter, 180-fs pulses.[43] The 2PA cross section value of **PE2** at 720 and 595 nm can also deviate because of its substantial dispersion, but, according to McKay et al., the 2PA spectrum is very broad and almost flat in the region 580 – 690 nm.[65] With all this information taken into account, a reasonable estimation of intrinsic **PE2** 2PA cross section would be several tens of GM near 595 nm.

First of all, even though our data present only a lower limit, and those of McKay et al. present an upper limit for σ_2, one can clearly see that all the molecules studied in the present work show substantially higher 2PA intensity (as presented in the last column of Table 3) than **PE2**. We do not present the data of Vestberg et al. in Table 3 because their σ_2 value does not correspond to 2PA maximum. Molecules **3** and **4** possess at least 1.4 and 2 times, respectively, stronger 2PA, first, because, due to substitution of phenyls with fluorenyls, they acquire longer and stronger conjugated backbone at their ends. Also, they carry strong symmetrically-attached electron-donating alkylamino groups, which were shown to drastically increase 2PA due to symmetrical charge transfer in the first excited state.[16] For platinum acetylide compounds this effect was demonstrated theoretically,[56] where diamino-substitution increased the 2PA strength of **PE1** by 5 times (cf. compounds **PE1-amino** and **PE1** in Table 3). It is also worth comparing **PE2** wit **1** and **2**. While the number of ethynyl bonds decreases in **1** and **2**, the replacement of phenylethynyl group at each side of **PE2** with benzthiazolylfluorenes and diphenylaminofluorenes in **1** and **2**, which represent strong electron acceptors or donors, repectively, and also the replacement of phenyl linker with more highly conjugated fluorene linker results in at least 2 and 3 times enhancement of integrated 2PA in **1** and **2**, respectively.

Summary and Conclusions

This investigation has focused on the synthesis and photophysical characterization of a series of platinum acetylide complexes that feature highly π-conjugated ligands substituted with π-donor or –acceptor moieties. The conjugated ligands impart the complexes with effective two-photon absorption properties, while the heavy metal platinum centers give rise to efficient intersystem crossing to afford long lived triplet states. Photophysical studies demonstrate that one-photon excitation of the chromophores produces an S_1 state that is delocalized across the two conjugated ligands, with weak (excitonic) coupling through the platinum center(s). The S_1 state is observed by ultrafast transient absorption and by its characteristic fluorescence. Intersystem crossing occurs rapidly ($k_{isc} \approx 10^{11}$ s^{-1}) to

produce the T_1 state, which is believed to be localized on a single conjugated fluorenyl ligand. The triplet state is strongly absorbing ($\varepsilon_{TT} > 5 \times 10^4$ $M^{-1}cm^{-1}$) and it is very long-lived ($\tau > 100$ μs).

Femtosecond pulses were used to characterize the two-photon absorption properties of the complexes, and as expected all of the chromophores are relatively efficient two photon absorbers in the visible and near-infrared region of the spectrum (600 – 800 nm). The complexes exhibit maximum 2PA at a shorter wavelength than 2λ for the 1PA band, consistent with the dominant 2PA transition arising from a two-photon allowed gerade-gerade transition. Nanosecond transient absorption experiments carried out on several of the complexes with excitation at 803 nm confirm that the long-lived triplet state can be produced efficiently via a sequence involving two-photon excitation to produce S_1 followed by intersystem crossing to afford T_1.

Acknowledgments. We are thankful for the support of this work by AFRL/ML Contracts F33615-99-C-5415 for D.G.M., F33615-03-D-5408 for D.M.K. and F33615-03-D-5421 for J.E.R. and J.E.S. and the Air Force Office of Scientific Research (AFOSR). We thank Evgeny Danilov and Prof. Michael Rodgers for use and help with the femtosecond transient absorption experiment at the Ohio Laboratory for Kinetic Spectrometry located at Bowling Green State University. We also thank Dr. Ramamurthi Kannan and Dr. Loon-Seng Tan at AFRL/MLBP for providing us with the ligands used for chromophores **1** and **2**. Rebane's group at Montana State University was supported by AFOSR grants FA9550-05-1-0357 and FA9550-05-1-0236. KSS and KYK acknowledge AFOSR for support (Grant No FA-9550-06-1-1084).

Supporting Information Available: Complete synthesis procedures, analytical data, NMR data as well as X-ray crystallographic file (CIF) of compounds 1 and 2 are available free of charge via the Internet at http://pubs.acs.org.

Figures.

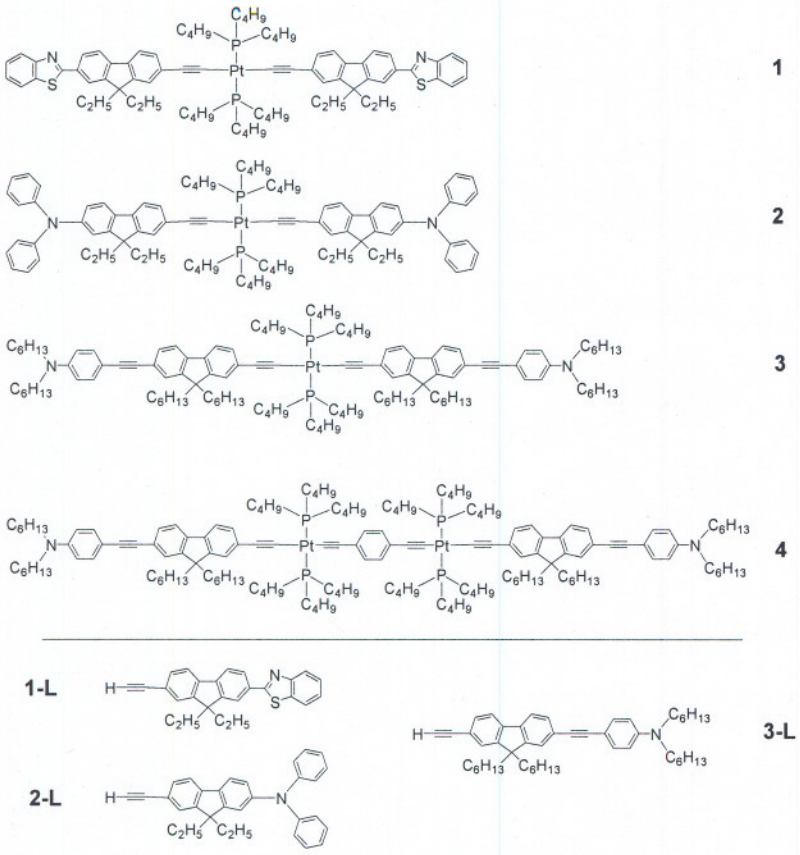

Figure 1. Chemical structures of platinum containing two-photon absorbing complexes **1**, **2**, **3**, and **4** and corresponding ligands **1-L**, **2-L**, and **3-L**.

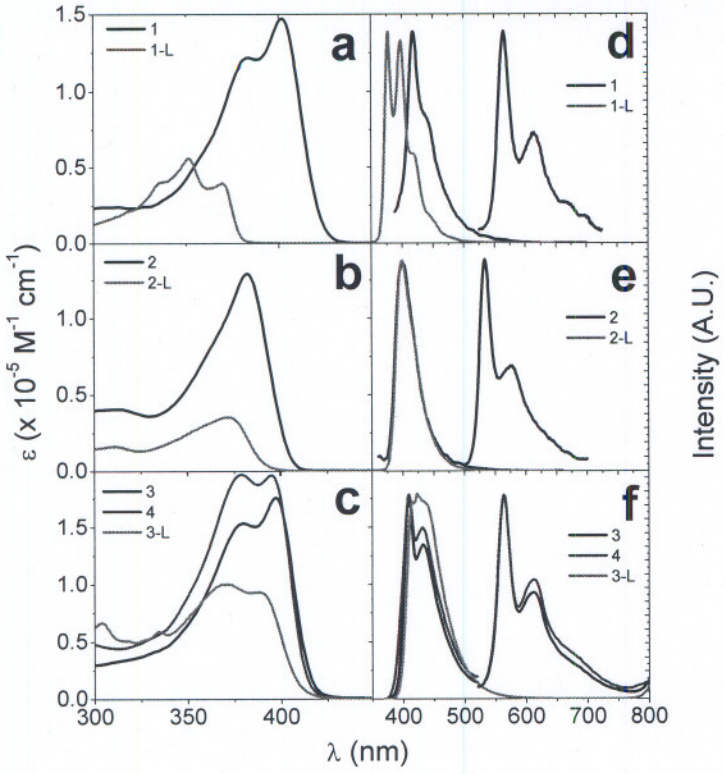

Figure 2. Quantified ground state absorption spectra of chromophores are shown in the left panels (a, b, and c). Data were obtained at room temperature (25 ^{o}C) in air saturated benzene. The right panels (d, e, and f) are emission spectra obtained upon 330 nm and 370 nm excitation in benzene at room temperature for the ligands and Pt chromophores, respectively. Samples were either air-saturated (fluorescence) or deoxygenated (phosphorescence) via three freeze-pump-thaw cycles. No room temperature phosphorescence was observed for **1-L**, **2-L**, and **3-L**.

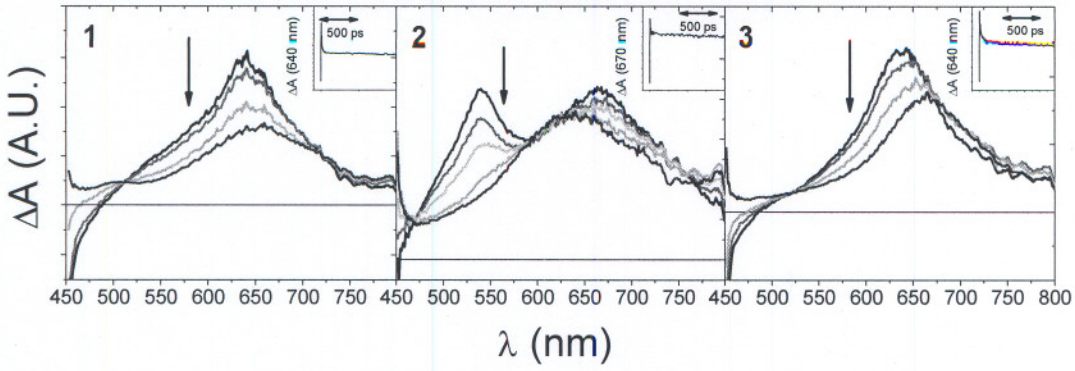

Figure 3. Femtosecond transient absorption spectra of **1** (32 μM), **2** (123 μM), and **3** (26 μM) in air-saturated benzene upon 400-nm excitation. Times shown are 0 ps (black), 1.5 ps (red), 3.4 ps (cyan – **2** only), 9.0 ps (green), and 48 ps (blue) after the 100 fs laser pulse. Similar spectral properties to **3** were observed for **4**.

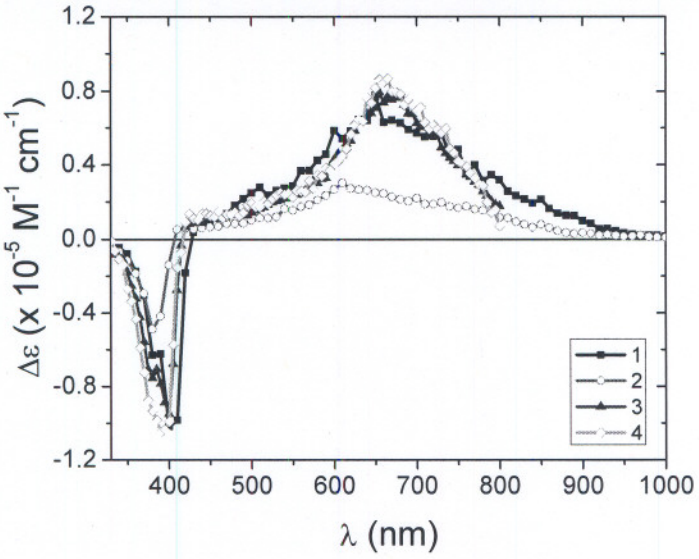

Figure 4. T_1-T_n absorption spectra observed after nanosecond pulsed 355-nm excitation of **1** (5.9 μM), **2** (2.5 μM), **3** (3.0 μM), and **4** (1.7 μM) in deoxygenated benzene. Samples were deoxygenated by the freeze-pump-thaw method. Molar extinction coefficients were obtained by using the method of relative actinometry.

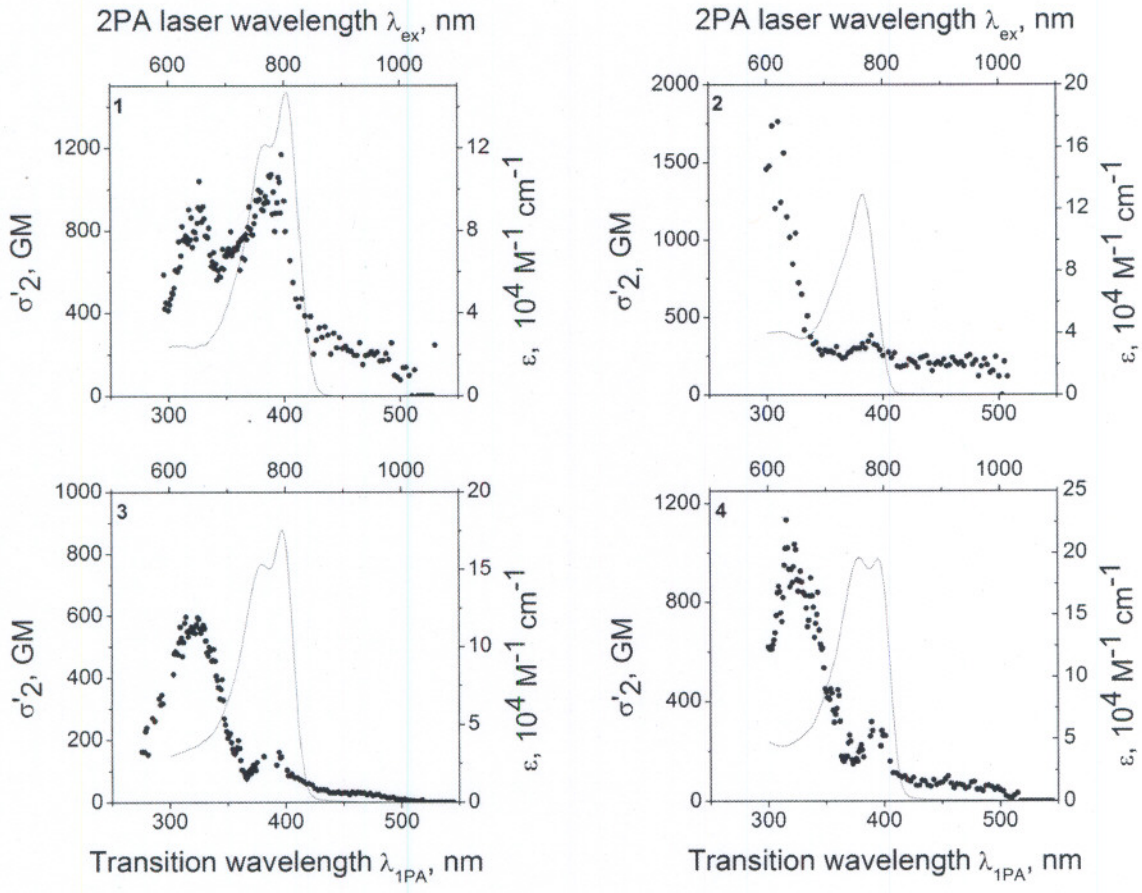

Figure 5. Two-photon absorption spectra of compounds **1-4** dissolved in benzene at ambient conditions (symbols). As described in the Experimental section, the samples were excited with 100-fs pulses with λ_{ex} = 550 - 1100 nm. The absolute two-photon absorption cross sections were measured using the sample fluorescence relative to a bis-diphenylaminostilbene solution in methylene chloride. This method gives the cross section value σ'_2, which, according to definition, is twice that would be obtained with nonlinear absorption techniques ($\sigma'_2 = 2\,\sigma_2$) [53]. One-photon absorption spectra (solid lines) are also shown for comparison. Bottom x-axis presents transition wavelength (which is equal to 1PA wavelength) and top x-axis presents laser wavelength, used for 2PA excitation.

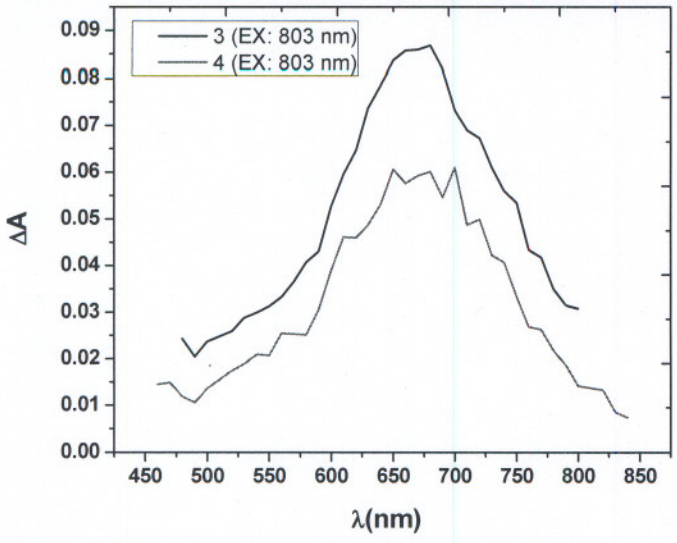

Figure 6. Examples of T_1-T_n absorption spectra produced by 5 ns, 803 nm pulsed excitation. All samples were prepared at 0.02 M in deoxygenated benzene. Deoxygenation was done with three freeze-pump-thaw cycles. Shown are data for compounds **3** and **4**.

Table 1. Summary of UV/Vis Absorbance and Emission Data in Benzene

	Abs_{max}	Fl_{max}	E_S(eV)	Φ_{fl}	Ph_{max}	Φ_{ph}
1	402 nm	418 nm	3.03	0.017(0.003)[a]	565 nm	0.018(0.002)
2	383 nm	399 nm	3.18	0.010(0.002)	534 nm	0.041(0.003)
3	397 nm	409 nm	3.08	0.038(0.004)	563 nm	0.071(0.007)[b]
4	397 nm	409 nm	3.08	0.037(0.004)	563 nm	0.084(0.008)[b]
1-L	351 nm	377 nm	3.30	0.692(0.004)	---	---
2-L	372 nm	399 nm	3.22	0.741(0.004)	---	---
3-L	371 nm	422 nm	3.14	0.710(0.004)	---	---

[a]Quantity in parenthesis is standard deviation.

[b]Estimated 10% standard deviation.

Table 2. Summary of Transient Absorbance Data in Benzene

	1	**2**	**3**	**4**
S_1-S_{nmax}	640 nm	540 nm	640 nm	640 nm
ε (M^{-1} cm^{-1})	136600	40600	107000	97000
τ_S (air)	23 ± 10 ps	42 ± 4 ps	48 ± 6 ps	12 ± 1 ps
T_1-T_{nmax}	670 nm	610 nm	670 nm	670 nm
ε (M^{-1} cm^{-1})	64300	30300	81000	83000
Φ_{ISC}	0.95 ± 0.02	0.94 ± 0.03	0.92 ± 0.05	0.94 ± 0.01
τ_T (air)	318 ns	44 ns	94 ns	99 ns
τ_T (deoxy)	126 μs	117 μs	213 μs	238 μs

Table 3. Summary of TPA Properties

molecule	$\sigma_{2,\ max}$ [GM]	$\lambda_{2PA,max}$ [nm]	Γ_f [cm^{-1}] (FWHM)	$\int\sigma_2 d(2\nu)$ [GM cm^{-1}]
1	415	649	4910	1.8×10^6
2	780	612	3570	2.5×10^6
PE1[b]	18.1	443	800[c]	1.5×10^4
3	290	634	4980	1.3×10^6
4	480	644	4540	2.0×10^6
PE1-amino[b]	90.2	495	800[c]	7.22×10^4
PE2[a]	235	630	~ 4000[a]	0.94×10^6
PE2[b]	37.6	457	800[c]	3.01×10^4

[a]From [42] [b]Quantum-chemical calculation from. [57] [c]FWHM, assumed value. [57]

Table 4. Nonlinear absorption parameters, relevant for higher-order multiphoton absorption processes.

molecule	σ_2 [GM] at 595 nm	σ_2 [GM] at 720 nm	σ_1^{T-T} [cm^2] (λ_{max}, nm)	$\Delta\lambda^{T-T}$ [nm] (FWHM)	τ_T (deoxy) [μs]
PE2	235[a] (27 ps, z-scan)	7[b] (180 fs, z-scan)	2.2×10^{-16} (600)[c]	200[d]	42[e]
1	210 (100 fs, fluo)	370 (100 fs, fluo)	2.4×10^{-16} (670)	220	126
2	720 (100 fs, fluo)	140 (100 fs, fluo)	1.2×10^{-16} (610)	250	117
3	155 (100 fs, fluo)	60 (100 fs, fluo)	3.1×10^{-16} (670)	170	213
4	300 (100 fs, fluo)	160 (100 fs, fluo)	3.2×10^{-16} (670)	160	238

[a]Ref. 6-8

[b]Ref. 27

[c]Ref. 9, 10

[d]Ref. 13

[e]Ref. 24

Schemes

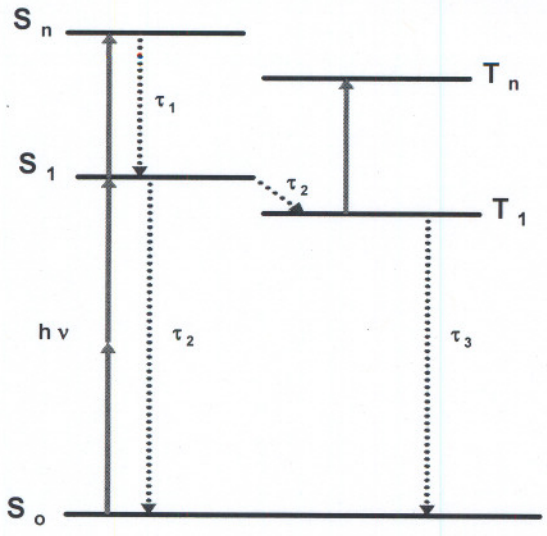

Scheme 1. Energy Level Diagram.

References

1. Parthenopoulos, D. A.; Rentzepis, P. M., *Science* **1989,** 249, 843.
2. Dvornikov, A. S.; Rentzepis, P. M., *Opt. Commun.* **1995,** 119, 341.
3. Bhawalkar, J. D.; He, G. S.; Prasad, P. N., *Rep. Prog. Phys.* **1996,** 59, 1041.
4. He, G. S.; Zhao, C. F.; Bhawalkar, J. D.; Prasad, P. N., *Appl. Phys. Lett.* **1995,** 78, 3703.
5. Zhao, C. F.; He, G. S.; Bhawalkar, J. D.; Park, C. K.; Prasad, P. N., *Chem. Mater.* **1995,** 7, 1979.
6. Fleitz, P. A.; Sutherland, R. A.; Strogkendl, F. P.; Larson, F. P.; Dalton, L. R., *SPIE Proc.* **1998,** 3472, 91.
7. He, G. S.; Bhawalkar, J. D.; Zhao, C. F.; Prasad, P. N., *Appl. Phys. Lett.* **1995,** 67, 2433.
8. Ehrlich, J. E.; Wu, X. L.; Lee, L. Y.; Hu, Z. Y.; Roeckel, H.; Marder, S. R.; Perry, J., *Opt. Lett.* **1997,** 22, 1843.
9. Kawata, S.; Sun, H. B.; Tanaka, T.; Takada, K., *Nature* **2001,** 412, 697-698.
10. Cumpston, B. H.; Ananthavel, S. P.; Barlow, S.; Dyer, D. L.; Ehrlich, J. E.; Erskine, L. L.; Heikal, A. A.; Kuebler, S. M.; Le, I. Y. S.; McCord-Maughon, D.; Qin, J.; Rockel, H.; Rumi, M.; Wu, X. L.; Marder, S. R.; Perry, J., *Nature* **1999,** 398, 51.
11. Denk, W.; Strickler, J. J.; Webb, W. W., *Science* **1990,** 248, 73.
12. Bhawalkar, J. D.; Kumar, N. D.; Zhao, C. F.; Prasad, P. N., *J. Clin.:aser Med. Surg.* **1997,** 15, 201.
13. Marder, S. R.; Gorman, C. B.; Meyers, F.; Perry, J.; Bourhill, G.; Bredas, J.-L.; Pierce, B. M., *Science* **1994,** 265, 632.
14. Prasad, P. N.; Reinhardt, B. A., *Chem. Mater.* **1990,** 2, 660.
15. Larson, E. J.; Friesen, L. A.; Johnson, C. K., *Chem. Phys. Lett.* **1997,** 265, 161.
16. Albota, M.; Beljonee, D.; Bredas, J.-L.; Ehrlich, J. E.; Fu, J.-Y.; Heikal, A. A.; Hess, S. E.; Kogej, T.; Levin, M. D.; Marder, S. R.; McCord-Maughon, D.; Perry, J.; Rockel, H.; Rumi, M.; Subramanian, G.; Webb, W. W.; Wu, X. L.; Xu, C., *Science* **1998,** 281, 1653.
17. Chung, S. J.; Kim, K. S.; Lin, T. C.; He, G. s.; Swiatkiewicz, J.; Prasad, P. N., *J. Phys. Chem. B* **1999,** 103, 10741.
18. Oberle, J.; Bramerie, L.; Jonusauskas, G.; Rullier, C., *Opt. Commun.* **1999,** 169, 325.
19. Belfield, K. D.; Hagan, D. J.; Van Stryland, E. W.; Schafer, K. J.; Negres, R. A., *Org. Lett.* **1999,** 1, 1575.
20. Kannan, R.; He, G. S.; Yuan, L.; Xu, F.; Prasad, P. N.; Dombroskie, A. G.; Reinhardt, B. A.; Baur, J. W.; Vaia, R. A.; Tan, L. S., *Chem. Mater.* **2001,** 13, 1896.

21. Mongrin, O.; Porres, L.; Katan, C.; Pons, T.; Mertz, J.; Blanchard-Desce, M., *Tetrahedron Lett.* **2003,** 44, 8121.

22. Brousmiche, D. W.; Serin, J. M.; Frechet, J. M. J.; He, G. S.; Lin, T. C.; Chung, S. J.; Prasad, P. N., *J. Am. Chem. Soc.* **2003,** 125, 1448.

23. Marder, S. R., *Chem. Commun.* **2006**, 131.

24. Rumi, M.; Ehrlich, J. E.; Heikal, A. A.; Perry, J. W.; Barlow, S.; Hu, Z. Y.; McCord-Maughon, D.; Parker, T. C.; Rockel, H.; Thayumanavan, S.; Marder, S. R.; Beljonne, D.; Bredas, J.-L., *J. Am. Chem. Soc.* **2000,** 122, 9500.

25. Kleinschmidt, J.; Rentsh, S.; Tottleben, W.; Wilhelmi, B., *Chem. Phys. Lett.* **1974,** 24, 133.

26. Sutherland, R. L.; Brant, M. C.; Heinrichs, J.; Rogers, J. E.; Slagle, J. E.; McLean, D. G.; Fleitz, P. A., *J. Opt. Soc. Am. B* **2005,** 22, 1939.

27. Sutherland, R. L.; McLean, D. G.; Brant, M. C.; Rogers, J. E.; Fleitz, P. A.; Urbas, A. M., *SPIE Proc.* **2006,** 6330, 633006.

28. Staromlynska, J.; McKay, T. J.; Bolger, J. A.; Davy, J. R., *J. Opt. Soc. Am. B* **1998,** 15, 1731.

29. Rogers, J. E.; Cooper, T. M.; Fleitz, P. A.; Glass, D. J.; McLean, D. G., *J. Phys. Chem. A* **2002,** 106, 10108-10115.

30. Liu, Y.; Jiang, S.; Glusac, K.; Powell, D. H.; Anderson, D. F.; Schanze, K. S., *J. Am. Chem. Soc.* **2002,** 124, 12412.

31. Haskins-Glusac, K.; Ghiviriga, I.; Abboud, K. A.; Schanze, K. S., *J. Phys. Chem. B* **2004,** 108, 4969.

32. Glimsdal, E.; Eriksson, A.; Vestberg, R.; Malmstrom, E.; Lindgren, M., *SPIE Proc.* **2005,** 5934, 1.

33. Reinhardt, B. A.; Brott, L. L.; Clarson, S. J.; Dillard, A. G.; Bhatt, J. C.; Kannan, R.; Yuan, L.; He, G. S.; Prasad, P. N., *Chem. Mater.* **1998,** 10, 1863.

34. Anemian, R.; andraud, C.; Nunzi, J.-M.; Morel, Y.; Baldeck, P. L., *SPIE Proc.* **2000,** 4106, 329.

35. Schroeder, R.; Ullrich, B., *Opt. Lett.* **2002,** 27, 1285.

36. Lee, K. S.; Yang, H.-K.; Lee, J.-H.; Kim, O.-K.; Woo, H. Y.; Choi, H.; Cha, M.; Blanchard-Desce, M., *SPIE Proc.* **2003,** 4991, 175.

37. Kannan, R.; He, G. S.; Lin, T. C.; Prasad, P. N.; Vaia, R. A.; Tan, L. S., *Chem. Mater.* **2004,** 16, 185.

38. Ma, W.; Wu, Y.; Han, J.; Gu, D.; Gan, F., *Chem. Phys. Lett.* **2005,** 403, 405.

39. Lin, T. C.; He, G. S.; Zheng, Q.; Prasad, P. N., *J. Mat. Chem.* **2006,** 16, 2490.

40. Glimsdal, E.; Carlsson, M.; Eliasson, B.; Lindgren, M., *SPIE Proc.* **2006,** 6401.

41. Glimsdal, E.; Carlsson, M.; Eliasson, B.; Minaev, B.; Lindgren, M., *J. Phys. Chem. A* **2006**.

42. McKay, T. J.; Staromlynska, J.; Wilson, P.; Davy, J. R., *J. Appl. Phys.* **1999,** 85, 1337.

43. Vestberg, R.; Westlund, R.; Ericksson, A.; Lopes, C.; Carlsson, M.; Eliasson, B.; Glimsdal, E.; Lindgren, M.; Malmstrom, E., *Macromol.* **2006,** 39, 2238.

44. Wang, Y. S.; Schanze, K. S., *Chem. Phys.* **1993,** 176, 305-319.

45. Nikolaitchik, A. V.; Korth, O.; Rodgers, M. A. J., *J. Phys. Chem. A* **1999,** 103, 7587.

46. Demas, J. N.; Crosby, G. A., *J. Phys. Chem.* **1971,** 75, 991.

47. Jones II, G.; Jackson, W. R.; Choi, C.; Bergmark, W. R., *J. Phys. Chem.* **1985,** 89, 294.

48. Thorn, N. B., *Chromophore Quenched Based Luminescence Probes for DNA*. University of Florida: Gainesville, 1995.

49. Carmichael, I.; Helman, W. P.; Hug, G. L., *J. Phys. Chem. Ref. Data* **1987,** 16, 239.

50. Amand, B.; Bensasson, R., *Chem. Phys. Lett.* **1975,** 34, 44.

51. Walters, K. A.; Schanze, K. S., *The Spectrum* **1998,** 11, 1.

52. Turro, N. J., *Modern Molecular Photochemistry*. Benjamin/Cummings: Menlo Park, 1978.

53. Murov, S. L.; Carmichael, I.; Hug, G. L., *Handbook of Photochemistry, 2nd ed.* Marcel Dekker, Inc.: New York, 1993.

54. Drobizhev, M.; Stepanenko, Y.; Dzenis, Y.; Karotki, A.; Rebane, A.; Taylor, P. N.; Anderson, H. L., *J. Phys. Chem. B* **2005,** 109, 7223.

55. Drobizhev, M.; Karotki, A.; Dzenis, Y.; Rebane, A.; Suo, Z.; Spangler, C. W., *J. Phys. Chem. B* **2003,** 107, 7540.

56. Connick, W. B.; Geiger, D.; Eisenberg, R., *Inorg. Chem.* **1999,** 38, 3264.

57. Norman, P.; Crostrand, P.; Ericsson, *J. Chem. Phys.* **2002,** 285, 207.

58. Cooper, T. M.; Krein, D. M.; Burke, A. R.; McLean, D. G.; Rogers, J. E.; Slagle, J. E., *J. Phys. Chem. A* **2006,** 110, 13370.

59. Rogers, J. E.; Hall, B. C.; Hufnagle, D. C.; Slagle, J. E.; Ault, A. P.; McLean, D. G.; Fleitz, P. A.; Cooper, T. M.,. *J. Chem. Phys.* **2005,** 122, 214708-214715.

60. Wasserberg, S. P.; Dudek, S. P.; Meskers, S. C. J.; Janssen, R. A. J., *Chem. Phys. Lett.* **2005,** 411, 273-277.

61. Wilson, J. S.; Chawdrury, N.; Al-Mandhary, M. R. A.; Younis, M.; Khan, M.; Raithby, P. R. K., A.; Friend, R. H., *J. Am. Chem. Soc.* **2001,** 123, 9412.

62. McCusker, J. K., *Acc. Chem. Res.* **2003,** 36, 876.

63. Bhasikuttan, A. C.; Suzuki, M.; Nakashima, S.; Okada, T., *J. Am. Chem. Soc.* **2002,** 124, 8398.

64. Ramakrishna, G.; Bhaskar, A.; Goodson, T., *J. Phys. Chem. B* **2006,** 110, 20872.

65. McKay, T. J.; Bolger, J. A.; Staromlynska, J.; Davy, J. R., *J. Chem. Phys.* **1998,** 108, 5537.

66. Staromlynska, J.; McKay, T. J.; Wilson, P., *J. Appl. Phys.* **2000,** 88, 1726.

67. McKay, T. J.; Staromlynska, J.; Davy, J. R.; Bolger, J. A., *J. Opt. Soc. Am. B* **2001,** 18, 358.

68. Cooper, T. M.; McLean, D. G.; Rogers, J. E., *Chem. Phys. Lett.* **2001,** 349, 31.

69. Cooper, T. M.; Blaudeau, J.-P.; Hall, B. C.; Rogers, J. E.; McLean, D. G.; Liu, Y.; Toscano, J. P., *Chem. Phys. Lett.* **2004,** 400, 239.

70. Silverman, E. E.; Cardolaccia, T.; Zhao, X.; Kim, K.-Y.; Haskins-Glusac, K.; Schanze, K. S., *Coord. Chem. Rev.* **2005,** 249, 1491.

71. Parola, S.; Ortenblad, M.; Chaput, F.; Desroshes, C.; Miele, P.; Baldeck, P. L.; Malmstrom, E.; Lindgren, M.; Eliasson, B.; Ericksson, A.; Lopes, C., *SPIE Proc.* **2005,** 5934, 1.

Supporting Information

Platinum Acetylide Two Photon Chromophores

[1,2]Joy E. Rogers, [1,3]Jonathan E. Slagle, [1,4]Douglas M. Krein, [1]Aaron R. Burke,

*[1,5]Benjamin C. Hall,[1,6] Albert Fratini, [1,7]Daniel G. McLean, and [1]Thomas M. Cooper**

[1]Materials and Manufacturing Directorate, Air Force Research Laboratory, Wright Patterson Air Force Base, OH 45433

[2]UES, Inc., Dayton, OH 45432

[3] AT&T Government Solutions, Dayton, OH 45324

[4]General Dynamics Information Technology, Dayton, OH 45431

[5]Universal Technology Corporation, Dayton, OH 45432

[6]Department of Chemistry, University of Dayton, Dayton, OH 45469

[7]Science Applications International Corporation, Dayton, OH 45431

*[8]Mikhail Drobijev, [8]Aleks Rebane**

[8]Physics Department, Montana State University, Bozeman, MT 59717

*[9]Kye-Young Kim, [9]Richard Farley, and [9]Kirk S. Schanze**

[9]Department of Chemistry, University of Florida, Gainesville, FL 32611

Contents

1. Structures

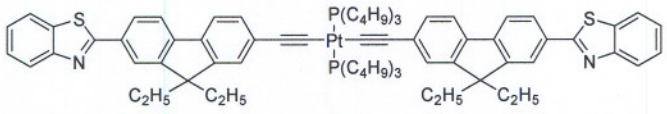

1

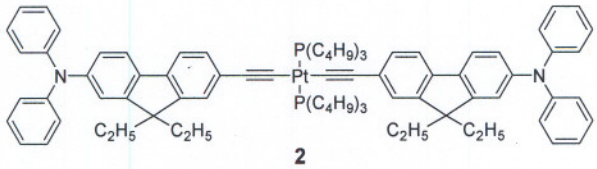

2

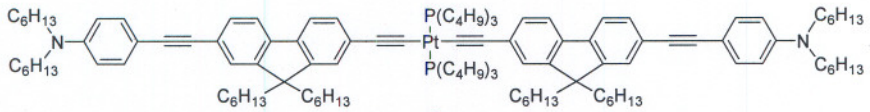

3

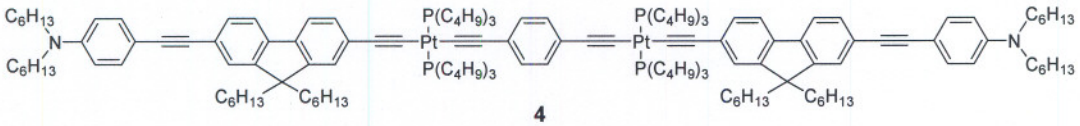

4

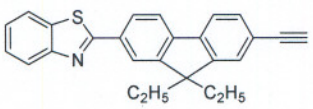

1-L

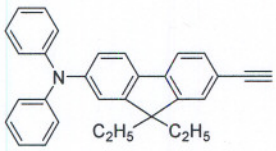

2-L

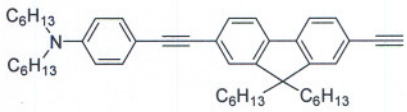

3-L

2. Synthetic Schemes

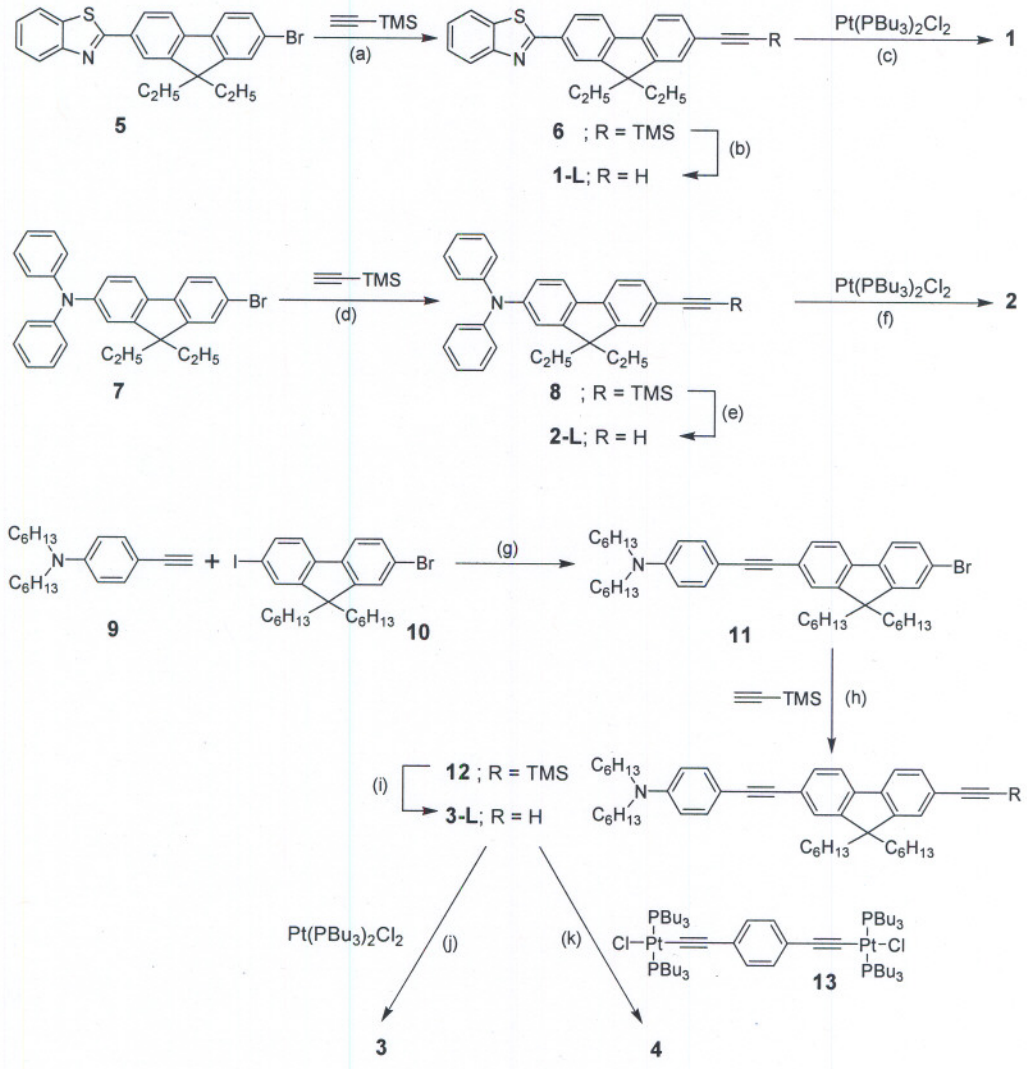

(a) $Pd(dba)_2$, CuI, PPh_3, Et_3N, 89%; (b) nBu_4NF, THF, MeOH, 96%; (c) CuI, Et_2NH, 85%; (d) $Pd(dba)_2$, CuI, PPh_3, Et_3N, 82%; (e) nBu_4NF, THF, MeOH, 94%; (f) CuI, Et_2NH, 81%; (g) $Pd(PPh_3)_4$, CuI, iPr_2NH, THF, 68%; (h) $Pd(PPh_3)_4$, CuI, iPr_2NH, DMF, 65 °C, 75%; (i) KF, MeOH, THF, 80%; (j) CuI, Et_2NH, THF, 85%; (k) CuI, Et_2NH, THF, 65%

3. Experimental Section

General Methods for Synthesis. All chemicals used for synthesis were of reagent grade and used without further purification unless otherwise noted. All reactions were carried out under argon atmosphere with freshly distilled solvents. Compounds **5** and **7**[1], **9**[2], **10**[3] and **13**[4] were synthesized according to literature procedure. Column chromatography was performed on silica gel (Merck®, Grade 7734). ^{1}H, ^{13}C and ^{31}P NMR spectra were recorded on a Varian Mercury 300 Spectrometer; ^{1}H and ^{13}C chemical shifts (δ) are reported in ppm and referenced to TMS or protonated solvent signals. ^{31}P NMR chemical shifts were referenced to 80% H_3PO_4. For compounds **1, 1-L, 2, 2-L, 6, 8**, high resolution mass spectra analyses were performed by the Ohio State University Mass Spectrometry and Proteomics Facility, and elemental analyses were performed by Chemsys, Inc. For compounds **3**, 3-L, **4**, **11** and **12**, mass spectra were recorded on Finnigan MAT95Q Hybrid Sector (EI, HRMS) or Bruker Reflex II (MALDI-TOF) mass spectrometers and elemental analyses were performed by University of Florida Spectroscopic Services.

---

[1] Kannan, R.; He, G. S.; Yuan, L.; Xu, F.; Prasad, P. N.; Dombroskie, A. G.; Reinhardt, B. A.; Baur, J. W.; Vaia, R. A.; Tan, L-S. *Chem. Mater*, **2001**, *13*, 1896.

[2] Kapplinger, C.; Beckert, R. *Synthesis*, **2002**, *13*, 1843.

[3] (a) Anemian, R.; Mulatier, J.-C.; Andraud, C.; Stephan, O.; Vial, J.-C. *Chem. Comm*. **2002**, *15*, 1608. (b) Kannan, R.; He, G. S.; Lin, T.-C.; Prasad, P. N.; Vaia, R. A.; Tan, L.-S. *Chem. Mater*. **2004**, *16*, 185.

[4] Schanze, K. S.; Silverman, E. E.; Zhao, X. *J. Phys. Chem. B,* **2005,** *109,* 18451.

Preparation of 2-(9,9-diethyl-2-(2-(trimethylsilyl)ethynyl)-9*H*-fluoren-7-yl)benzo[*d*] thiazole

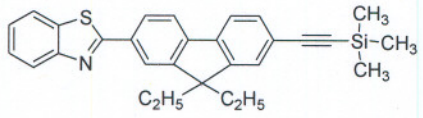

(6)

A stirred solution of 2-(7-Bromo-9,9-diethylfluoren-2-yl) benzothiazole **5** (8.69 g, 20.0 mmol), in NEt_3 (200 mL) was deoxygenated *via* freeze-pump-thaw (3x, liq. N_2, 10 mTorr), purged with argon, and allowed to return to room temperature. To this mixture was added trimethylsilylacetylene (2.95 g, 30.0 mmol, 4.25 mL) *via* syringe, followed by PPh_3 (0.21g, 0.80 mmol) , $Pd(dba)_2$ (0.23 g, 0.40 mmol) and CuI (0.08g, 0.40 mmol). This mixture was then sealed and stirred at 85 °C overnight. This mixture was then reduced *in vacuo*, diluted with CH_2Cl_2 (50 mL), and flash-filtered through silica gel (CH_2Cl_2/Hexanes, 1:1). The filtrate was again concentrated *in vacuo* to afford a dark red-orange oil. Purification *via* column chromatography on silica gel (CH_2Cl_2/Hexanes, 1:4) gave **6** (7.88 g, 89%) as a cream-colored solid: mp 179-180 °C. ^{1}H NMR (300 MHz, $CDCl_3$) δ 8.15 (d, J = 1.5 Hz, 1H), 8.12 (d, J = 8.1 Hz, 1H), 8.05 (dd, J = 8.1, 1.5 Hz, 1H), 7.93 (d, J = 7.8 Hz, 1H), 7.78 (d, J = 7.8 Hz, 1H), 7.70 (dd, J = 8.0, 1.0 Hz, 1H), 7.55-7.50 (m, 3H), 7.41 (dt, J = 7.8, 1.0 Hz, 1H), 2.15 (two sets of diastereotopic quartets, J = 19.5, 7.5 Hz, 4H), 0.36 (t, J = 7.5 Hz, 6H), 0.33 (s, 9H); ^{13}C NMR (75 MHz, $CDCl_3$) δ 168.76, 154.48, 151.41, 150.80, 144.06, 141.24, 135.26, 133.01, 131.60, 127.52, 126.75, 126.63, 125.40, 123.34, 122.55, 121.84, 121.79, 120.70, 120.34, 106.18, 94.92, 56.88, 32.97, 8.75, 0.31; IR (KBr) ν 2095 cm^{-1}; HRMS (TOF-MS-ES+) calcd [M + H] 452.1868; found [M + H] 452.1864; Anal. Calcd. for $C_{29}H_{19}NSiS$: C, 77.11%; H, 6.47%; N, 3.10%. Found: C, 77.48%; H, 6.70%; N, 3.17%.

Preparation of 2-(9,9-diethyl-9*H*-fluoren-7-yl)benzo[*d*]thiazole

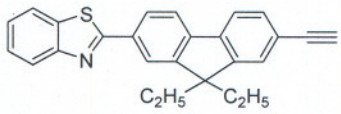

(1-L)

To a stirred solution of **6** (7.73 g, 17.5 mmol) in THF (150 mL) and MeOH (25 mL) was added tetrabutylammonium fluoride hydrate (5.72 g, 21.9 mmol). The mixture was stirred under argon at room temperature for 8 h. The solvent was removed *in vacuo* and the resulting dark oil was absorbed onto silica gel. Purification *via* column chromatography on silica gel (CH_2Cl_2/Hexanes, 1:4) gave **1-L** (6.21 g, 96%) as a cream-colored solid: mp 122-123 °C. ^{1}H NMR (300 MHz, $CDCl_3$) δ 8.17 (d, J = 1.5 Hz, 1H), 8.13 (dd, J = 8.1, 1.0 Hz, 1H), 8.07 (dd, J = 8.1, 1.5 Hz, 1H), 7.94 (dd, J = 7.8, 1.0 Hz, 1H), 7.81 (d, J = 8.1 Hz, 1H), 7.73 (dd, J = 7.8, 1.0 Hz, 1H), 7.57-7.51 (m, 3H), 7.42 (dt, J = 7.8, 1.0 Hz, 1H), 3.21 (s, 1H), 2.15 (two sets of diastereotopic quart., J = 19.5, 7.5 Hz, 4H), 0.36 (t, J = 7.5 Hz, 6H); ^{13}C NMR (75 MHz, $CDCl_3$) δ 168.71, 154.48, 151.43, 150.91, 143.91, 141.51, 135.27, 133.14, 131.65, 127.55, 126.99, 126.64, 125.43, 123.36, 121.88, 121.86, 121.51, 120.76, 120.44, 84.71, 77.87 (d, J = 3.0 Hz), 56.86, 32.93, 8.77; IR (KBr) ν 3293, 2103 cm^{-1}; HRMS (TOF-MS-ES+) calcd [M + H] 380.1473; found [M + H] 380.1470; Anal. Calcd. for $C_{26}H_{21}NS$: C, 82.28%; H, 5.58%; N, 3.69%. Found: C, 82.01%; H, 5.81%; N, 3.78%.

Preparation of *trans*-bis-(tributylphosphine)-bis-(2-(9,9-diethyl-9*H*-fluoren-7-yl)benzo [*d*]thiazole) platinum

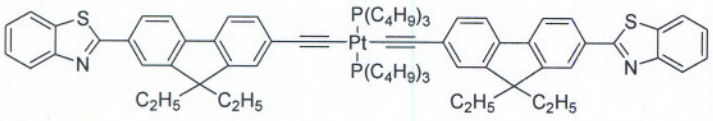

(1)

A solution of **1-L** (1.22 g, 3.30 mmol) and $PtCl_2(PBu_3)_2$ (2.01 g, 3.00 mmol) in Et_3N (50 mL) was deoxygenated *via* freeze-pump-thaw (3x, liq. N_2, 10 mTorr), purged with argon, and allowed to return to room temperature. To this mixture was added CuI (0.03g, 0.15 mmol). This mixture was then sealed and stirred at 85 °C overnight. This mixture was then reduced *in vacuo*, diluted with CH_2Cl_2 (10 mL), absorbed onto silica and flash-filtered through silica gel (CH_2Cl_2/Hexanes, 1:1). The filtrate was again concentrated *in vacuo* to afford a yellow oil. Purification *via* column chromatography on silica gel (CH_2Cl_2/Hexanes, 1:3) gave **1** (3.41 g, 85%) as a light yellow solid: mp 205-206 °C (dec.). ^{1}H NMR (300 MHz, $CDCl_3$) δ 8.13 (d, J = 1.2 Hz, 2H), 8.11 (dd, J = 8.1, 1.0 Hz, 2H), 8.04 (dd, J = 8.1, 1.5 Hz, 2H), 7.94 (dd, J = 7.5, 1.0 Hz, 2H), 7.75 (d, J = 8.1 Hz, 2H), 7.64 (d, J = 8.5 Hz, 2H), 7.53 (dt, J = 8.4, 1.0 Hz, 2H), 7.41 (dt, J = 7.5, 1.0 Hz, 2H), 7.34-7.29 (m, 4H), 2.33-2.20 (m, 12H), 2.12 (two sets of diastereotopic quart., J = 19.5, 7.5 Hz, 8H), 1.78-1.64 (m, 12H), 1.52 (sextet, J = 7.4 Hz, 12H), 0.99 (t, J = 7.4 Hz, 18H), 0.38 (t, J = 7.5 Hz, 12H); ^{13}C NMR (75 MHz, $CDCl_3$) δ 169.17, 154.53, 151.03, 150.59, 145.15, 137.75, 135.21, 131.91, 130.13, 128.99, 127.48, 126.53, 125.68, 125.22, 123.20, 121.80, 121.70, 120.07, 119.92, 110.55, 109.93 (t, $J^2_{P\text{-}C}$ = 14.6 Hz), 56.52, 33.08, 26.67, 24.74 (t, $J^1_{P\text{-}C}$ = 6.8 Hz), 24.32 (t, $J^2_{P\text{-}C}$ = 17.1 Hz), 14.11, 8.76: ^{31}P NMR (121 MHz) δ 4.19 ($J_{Pt\text{-}P}$ = 2355 Hz); IR

(KBr) ν 2095 cm^{-1}; HRMS (ESI-MS) calcd [M + H] 1355.6034; found [M + H] 1355.6012; Anal. Calcd. for $C_{76}H_{74}N_2P_2S_2Pt \cdot 0.25CH_2Cl_2$: C, 66.46%; H, 6.91%; N, 2.03%. Found: C, 66.52%; H, 6.94%; N, 1.92%.

Preparation of 9,9-diethyl-7-(2-trimethylsilyl)ethynyl)-*N*,*N*-diphenyl-9*H*-fluoren-2-amine

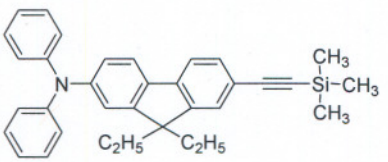

(8)

A stirred solution of (7-Bromo-9,9-diethylfluoren-2-yl)diphenylamine **7** (9.39 g, 20.0 mmol), in NEt_3 (200 mL) was deoxygenated *via* freeze-pump-thaw (3x, liq. N_2, 10 mTorr), purged with argon, and allowed to return to room temperature. To this mixture was added trimethylsilylacetylene (2.95 g, 30.0 mmol, 4.25 mL) *via* syringe, followed by PPh_3 (0.21g, 0.80 mmol) , $Pd(dba)_2$ (0.23 g, 0.40 mmol) and CuI (0.08g, 0.40 mmol). This mixture was then sealed and stirred at 85 °C overnight. This mixture was then reduced *in vacuo*, diluted with CH_2Cl_2 (50 mL), and flash-filtered through silica gel (CH_2Cl_2/Hexanes, 1:1). The filtrate was again concentrated *in vacuo* to afford a dark orange oil. Purification *via* column chromatography on silica gel (CH_2Cl_2/Hexanes, 1:5) gave **8** (8.55 g, 82%) as a white solid: mp 194-195 °C. ^{1}H NMR (300 MHz, $CDCl_3$) δ 7.48 (dd, J = 7.8, 1.5 Hz, 1H), 7.44 (br. s, 1H), 7.32-7.27 (m, 4H), 7.18-7.12 (m, 5H), 7.09-7.03 (m, 3H), 1.95 (two sets of diastereotopic quartets, J = 12.8, 7.5 Hz, 4H), 0.37 (t, J = 7.5 Hz, 6H), 0.32 (s, 9H); ^{13}C NMR (75 MHz, $CDCl_3$) δ 151.93, 149.99, 148.19, 147.95, 142.17, 136.06, 131.52, 129.49, 126.51, 124.25, 123.74, 122.93, 120.99, 120.64, 119.30, 119.09, 106.63, 93.93, 56.39, 32.87, 8.76, 0.36; IR (KBr) ν 2152 cm^{-1}; HRMS (ESI-MS) calcd [M + Na] 508.2436; found [M + Na] 508.2435; Anal. Calcd. for $C_{34}H_{35}NSi$: C, 84.07%; H, 7.26%; N, 2.88%. Found: C, 83.76%; H, 7.26%; N, 2.71%.

Preparation of 9,9-diethyl-7-ethynyl-*N*,*N*-diphenyl-9*H*-fluoren-2-amine

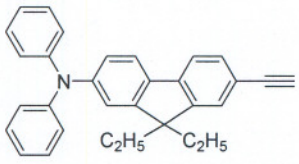

(2-L)

To a stirred solution of **8** (8.50 g, 17.5 mmol) in THF (150 mL) and MeOH (25 mL) was added tetrabutylammonium fluoride hydrate (5.72 g, 21.9 mmol). The mixture was stirred under argon at room temperature for 8 h. The solvent was removed in vacuo and the resulting dark oil was absorbed onto silica gel. Purification *via* column chromatography on silica gel (CH_2Cl_2/Hexanes, 1:4) gave **2-L** (6.79 g, 94%) as a cream-colored solid: mp 138-139 °C. ^{1}H NMR (300 MHz, $CDCl_3$) δ 7.60 (d, J = 1.2 Hz, 1H), 7.57 (d, J = 1.6 Hz, 1H), 7.50 (dd, J = 7.8, 1.5 Hz, 1H), 7.46 (br. s, 1H), 7.32-7.27 (m, 4H), 7.18-7.12 (m, 5H), 7.09-7.03 (m, 3H), 3.15 (s, 1H), 1.95 (two sets of diastereotopic quartets, J = 12.8, 7.5 Hz, 4H), 0.38 (t, J = 7.5 Hz, 6H); ^{13}C NMR (75 MHz, $CDCl_3$) δ 151.95, 150.10, 148.17, 148.05, 142.42, 135.88, 131.54, 129.50, 126.72, 124.29, 123.69, 122.97, 121.04, 119.57, 119.24, 119.17, 85.08, 77.05 (d, J = 3.0 Hz), 56.37, 32.83, 8.77; IR (KBr) ν 3290, 2104 cm^{-1}; HRMS (ESI-MS) calcd [M + Na] 436.2041; found [M + Na] 436.2045; Anal. Calcd. for $C_{29}H_{19}NSiS$: C, 90.03%; H, 6.58%; N, 3.39%. Found: C, 89.76%; H, 6.98%; N, 3.24%.

Preparation of *trans*-bis(tributylphosphine)-bis(9,9-diethyl-7-ethynyl-*N*,*N*-diphenyl-9*H*-fluoren-2-amine) platinum

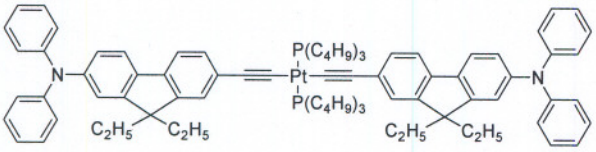

(2)

A solution of **2-L** (1.36 g, 3.30 mmol) and $PtCl_2(PBu_3)_2$ (2.01 g, 3.00 mmol) in Et_3N (50 mL) was deoxygenated *via* freeze-pump-thaw (3x, liq. N_2, 10 mTorr), purged with argon, and allowed to return to room temperature. To this mixture was added CuI (0.03g, 0.15 mmol). This mixture was then sealed and stirred at 85 °C overnight. This mixture was then reduced *in vacuo*, diluted with CH_2Cl_2 (10 mL), absorbed onto silica and flash-filtered through silica gel (CH_2Cl_2/Hexanes, 1:1). The filtrate was again concentrated *in vacuo* to afford a yellow oil. Purification *via* column chromatography on silica gel (CH_2Cl_2/Hexanes, 1:2) gave **2** (3.46 g, 81%) as a yellow-orange solid: mp 172-173 °C (dec.). ^{1}H NMR (300 MHz, $CDCl_3$) δ 7.55 (br. s, 1H), 7.53 (br. s, 1H), 7.51 (br. s, 1H), 7.48 (br. s, 1H), 7.30-7.25 (m, 12H), 7.15-7.10 (m, 10H), 7.06-7.00 (m, 6H)), 2.28-2.19 (m, 12H), 1.91 (two sets of diastereotopic quart., J = 19.5, 7.5 Hz, 8H), 1.76-1.64 (m, 12H), 1.51 (sextet, J = 7.4 Hz, 12H), 0.98 (t, J = 7.4 Hz, 18H), 0.39 (t, J = 7.5 Hz, 12H); ^{13}C NMR (75 MHz, $CDCl_3$) δ 151.55, 149.70, 148.35, 146.80, 138.55, 137.40, 129.96, 129.39, 127.24, 125.56, 124.14, 123.90, 122.54, 120.23, 119.91, 118.85, 110.43, 108.31 (t, $J^2_{P\text{-}C}$ = 15.0 Hz), 56.10, 32.99, 26.65, 24.73 (t, $J^1_{P\text{-}C}$ = 7.0 Hz), 24.28 (t, $J^2_{P\text{-}C}$ = 17.1 Hz), 14.11, 8.76: ^{31}P NMR (121 MHz) δ 4.00 ($J_{Pt\text{-}P}$ = 2360 Hz); IR (KBr) ν 2096 cm^{-1}; HRMS (ESI-MS) calcd [M + H] 1422.7458;

found [M + H] 1422.7467; Anal. Calcd. for $C_{86}H_{106}N_2P_2Pt \cdot 0.50CH_2Cl_2$: C, 70.81%; H, 7.35%; N, 1.91%. Found: C, 71.11%; H, 7.29%; N, 1.80%.

Preparation of 4 - (2- (2 – bromo -9, 9 –dihexyl - 9H-fluoren -7-yl)ethynyl)- N,N - dihexylbenzenamine

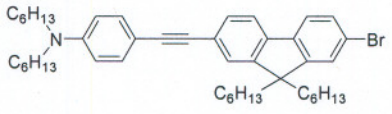

(11)

A stirred solution of 4-ethynyl-N,N-dihexylaniline **9** (3.00 g, 10.5 mmol), 2-bromo-7-iodo-9,9-dihexylfluorene **10** (5.66 g, 10.5 mmol) in iPr_2NH/THF (20 mL, 1:1 v/v) was degassed with argon for 30 min. To this mixture was added CuI (40 mg, 0.21 mmol) followed by $Pd(PPh_3)_4$ (0.243 g, 0.21 mmol). The mixture was stirred at room temperature for 12h. To this mixture was then added H_2O (50 mL) and the resulting solution was extracted with diethyl ether (50 mL x 3). The combined organic layer was washed with water (50 mL × 2), dried over Na_2SO_4 and the solvent was removed *in vacuo* to give a dark yellow oil. Column chromatography on silica gel (CH_2Cl_2/hexane, 1:3) gave the desired product **11** as a yellow solid (4.98 g, 68%): ^{1}H NMR (300 MHz, CD_2Cl_2) δ 7.65 (d, J = 8.5 Hz, 1H), 7.57 (d, J = 8.1 Hz, 1H), 7.51-7.45 (m, 4H), 7.37 (d, J = 9.0 Hz, 2H), 6.62 (d, J = 9.0 Hz, 2H), 3.30 (t, J = 7.7 Hz, 4H), 1.98 (m, 4H), 1.60 (m, 4H), 1.35 (br s, 12H), 1.20-1.02 (m, 12H), 0.92 (t, J = 6.7 Hz, 6H), 0.79 (t, J = 6.9 Hz, 6H), 0.61 (m, 4H); ^{13}C NMR (75 MHz, CD_2Cl_2) δ 153.87, 151.05, 148.71, 140.37, 139.98, 133.30, 130.70, 130.56, 126.81, 126.12, 123.77, 121.75, 121.72, 120.27, 111.83, 108.96, 91.89, 88.44, 56.05, 51.50, 40.89, 32.33, 32.15, 30.25, 27.75, 27.37, 24.35, 23.31, 23.20, 14.44, 14.37; IR (KBr) ν 2928, 2193 cm^{-1}; HRMS (ESI-FTICR-MS) calcd [M + H]; 696.4138; found [M + H] 696.4131.

Preparation of N,N-dihexyl-4-(2-(9,9-dihexyl-2-(2-(trimethylsilyl)ethynyl)-9H-fluoren-7-yl)ethynyl)benzenamine

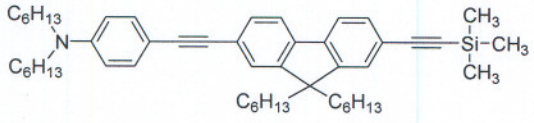

(**12**)

A stirred solution of **11** (5.0 g, 7.2 mmol), $Pd(PPh_3)_4$ (166 mg, 0.144 mmol) and CuI (27 mg, 0.14 mol) in iPr_2NH/ DMF (25 mL, 1:1 v/v) was degassed with argon for 30 min. To this mixture was added trimethylsilylacetylene (1.1 g, 11 mmol) *via* syringe and stirred at 65 °C for 12 h. To this mixture was then added H_2O (70 mL) and the organic layer was extracted with diethyl ether (50 mL x 3). The combined organic layer was washed with water (50 mL × 2), dried over Na_2SO_4 and the solvent was removed in vacuo to give a brown oil. Column chromatography on silica gel (CH_2Cl_2/hexane, 1; 3) gave **12** as a yellow solid (3.86 g, 75%): ^{1}H NMR (300 MHz, $CDCl_3$) δ 7.62 (d, J = 7.6 Hz, 1H), 7.59 (d, J = 7.6 Hz, 1H), 7.48-7.42 (m, 4H), 7.39 (d, J = 9.0 Hz, 2H), 6.58 (d, J = 9.0 Hz, 2H), 3.28 (t, J = 7.7 Hz, 4H), 1.94 (m, 4H), 1.58 (m, 4H), 1.32 (br s, 12H), 1.10 (m, 4H), 1.05-1.01 (m, 8H), 0.91 (t, J = 6.6 Hz, 6H), 0.77 (t, J = 6.7 Hz, 6H), 0.57 (m, 4H), 0.29 (s, 9H) ; ^{13}C NMR (75 MHz, $CDCl_3$) δ 150.98, 150.83, 147.94, 141.19, 139.67, 132.86, 131.17, 130.32, 126.17, 125.50, 123.13, 121.31, 119.85, 119.57, 111.19, 108.66, 106.25, 93.99, 91.32, 88.08, 55.15, 50.95, 40.43, 31.70, 31.55, 29.71, 27.19, 26.80, 23.65, 22.67, 22.62, 14.03, 13.99, 0.055; IR (KBr) ν 2928, 2194, 2153 cm^{-1}; HRMS (ESI-FTICR-MS) cacld [M + H]; 714.5429; found [M + H] 714.5398.

Preparation of 4-(2-(2-ethynyl-9,9-dihexyl-9H-fluoren-7-yl)ethynyl)-N,N-dihexylbenzenamine

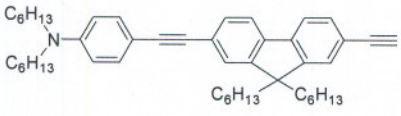

(3-L)

To a stirred solution of **12** (3.5 g, 4.9 mmol) in THF/MeOH (15 mL, 2:1 v/v) was added potassium fluoride (0.56 g, 9.8 mmol). The mixture was stirred under nitrogen at room temperature for 2 h. The solvent was removed under the reduced pressure and the resulting oil was taken up in CH_2Cl_2 (50 mL), washed with H_2O (20 mL x 2), dried over $MgSO_4$, and concentrated *in vacuo* to give a dark brown oil. Column chromatography on silica gel (CH_2Cl_2/hexane, 1:3) gave **3-L** as a yellow solid (2.52 g, 80%): ^{1}H NMR (300 MHz, $CDCl_3$) δ 7.62 (dd, J = 7.8 and 2.4 Hz, 1H), 7.61 (dd, J = 7.6 and 2.4 Hz, 1H), 7.49-7.46 (m, 4H), 7.39 (d, J = 8.8 Hz, 2H), 6.58 (d, J = 8.8 Hz, 2H). 3.28 (t, J = 7.7 Hz, 4H), 3.15 (s, 1H), 1.95 (m, 4H), 1.59 (m, 4H), 1.32 (s, 12H), 1.15-1.10 (m, 4H), 1.05-1.02 (m, 8H), 0.91 (t, J = 6.7 Hz, 6H), 0.77 (t, J = 7.2 Hz, 6H), 0.58 (m, 4H); ^{13}C NMR (75 MHz, CD_2Cl_2) δ 151.56, 151.44, 148.53, 141.87, 139.99, 133.12, 131.52, 130.51, 126.93, 125.94, 123.74, 120.80, 120.38, 120.09, 111.64, 108.76, 91.81, 88.29, 84.87, 77.44, 55.60, 51.31, 40.71, 32.13, 31.97, 30.08, 27.56, 27.17, 24.18, 23.11, 23.01, 14.24, 14.17; IR (KBr) ν 2928, 2192 cm^{-1}; HRMS (ESI-FTICR-MS) cacld [M + H]; 642.5033; found [M + H] 642.5000.

Preparation of *trans*-bis-(tributylphosphine)-bis-(4-(2-(2-ethynyl-9,9-dihexyl-9H-fluoren-7-yl)ethynyl)-N,N-dihexylbenzenamine)-platinum

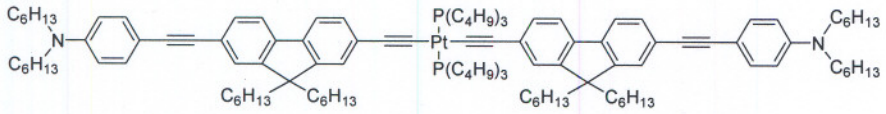

3

A solution of **3-L** (0.64 g, 0.99 mmol) and $PtCl_2(PBu_3)_2$ (0.30 g, 0.45 mmol) in Et_2NH/THF (10 mL, 1:1 v/v) was degassed with argon for 20 min and added CuI (3 mg). The mixture was stirred at room temperature for 7h. The solvent was removed *in vacuo* and the resulting waxy solid was preadsorbed onto silica gel (1.0 g). Column chromatography on silica gel (CH_2Cl_2/hexane, 1:2) afforded **3** as a yellow solid (0.72 g, 85%): mp 127-129 °C; ^{1}H NMR (300 MHz, $CDCl_3$) δ 7.56 (d, J = 7.8 Hz, 2H), 7.51 (d, J = 8.1 Hz, 2H), 7.45-7.42 (m, 4H), 7.39 (d, J = 8.8 Hz, 4H), 7.26-7.23 (m, 4H), 6.58 (d, J = 9.0 Hz, 4H), 3.28 (t, J = 7.8 Hz, 8H), 2.21 (m, 12H), 1.91 (m, 8H), 1.67 (m, 12H), 1.59 (m, 8H), 1.47 (m, 12H), 1.33 (br m), 24H), 1.12 (m, 8H), 1.04 (m, 16H), 0.98-0.88 (m, 30H), 0.80 (t, J = 7.1 Hz, 12H), 0.63 (m, 8H); ^{13}C NMR (75 MHz, $CDCl_3$) δ 150.62, 150.55, 147.82, 140.68, 137.67, 132.78, 130.20, 129.66, 127.75, 125.39, 125.15, 121.78, 119.26, 119.12, 111.18, 110.28, 108.88, 108.51 ($J_{C\text{-}P}$ = 14.9 Hz), 90.65, 88.32, 54.78, 50.94, 40.62, 31.69, 31.57, 29.80, 27.18, 26.79, 26.38, 24.45 ($J_{C\text{-}P}$ = 6.7 Hz), 23.98 ($J_{C\text{-}P}$ = 17.2 Hz), 23.68, 22.94, 22.93, 14.02, 13.99, 13.83; ^{31}P NMR (121 MHz, $CDCl_3$) δ 4.01 ($J_{Pt\text{-}P}$ = 2357 Hz); IR (KBr) ν 2955, 2095 cm^{-1}; HRMS (ESI-FTICR-MS) calcd [M + H]; 1882.3216; found [M + H] 1882.2855: Anal. cald. for $C_{118}H_{178}N_2P_2Pt$ (%): C, 75.32; H, 9.53; N, 1.49; found C, 75.24; H, 9.89; N, 1.43.

Preparation of *trans*-bis(tributylphosphine)(4-(2-(2-ethynyl-9,9-dihexyl-9H-fluoren-7-yl)ethynyl)-N,N-dihexylbenzenamine)[(*trans*-bis(tributylphosphine)(1,4-diethynylbenzene)(4-(2-(2-ethynyl-9,9-dihexyl-9H-fluoren-7-yl)ethynyl)-N,N-dihexylbenzenamine)platinum]platinum

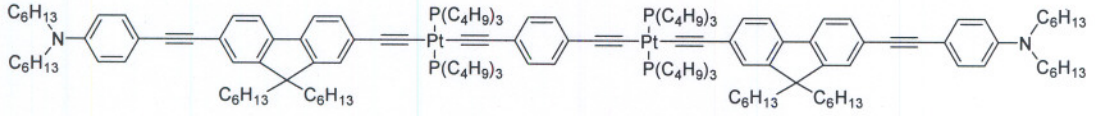

4

Platinum complex **13** (0.55 g, 0.39 mmol) and **3-L** (0.54 g, 0.84 mmol) were dissolved in Et_2NH/THF (10 mL, 1:1 v/v) and the mixture was degassed with argon for 20 min. To this mixture was added CuI (3 mg) and the resulting mixture was stirred at room temperature for 10 h. The solvent was removed *in vacuo* and the resulting waxy solid was preadsorbed onto silica gel (1.0 g). Column chromatography on silica gel (CH_2Cl_2/hexane, 2:3) afforded **4** as a yellow solid (0.66 g, 65%): mp 133-134 °C; ^{1}H NMR (300 MHz, CD_2Cl_2) δ 7.61 (d, J = 8.5 Hz, 2H), 7.56 (d, J = 8.5 Hz, 2H), 7.46 (s, 2H), 7.45 (d, J = 8.4 Hz, 2H), 7.38 (d, J = 8.8 Hz, 4H), 7.26 (s, 2H), 7.25 (d, J = 8.4 Hz, 2H), 7.12 (s, 4H), 6.63 (d, J = 9.0 Hz, 4H), 3.32 (t, J = 7.5 Hz, 8H), 2.19 (m, 24H), 1.97 (m, 8H), 1.68-1.61 (m, 32H), 1.52 (m, 24H), 1.36 (br m, 24H), 1.14 (m, 8H), 1.10-1.08 (m, 16H), 1.00-0.91 (m, 48H), 0.80 (t, J = 6.9 Hz, 12H), 0.64 (m, 8H); ^{13}C NMR (75 MHz, CD_2Cl_2) δ 151.37, 151.29, 148.61, 141.31, 138.11, 133.21, 130.84, 130.56, 130.16, 128.80, 126.24, 125.98, 125.66, 122.47, 119.89, 119.73, 111.82, 110.56, 109.99 ($J_{C\text{-}P}$ = 14.3 Hz), 109.69, 109.55 ($J_{C\text{-}P}$ = 14.6 Hz), 109.15, 91.29, 88.71, 55.43, 51.49, 41.14, 32.31, 32.22, 30.38, 27.74, 27.35, 26.97, 25.04 ($J_{C\text{-}P}$ = 6.7 Hz),

24.55 ($J_{C\text{-}P}$ = 17.2 Hz), 24.42, 23.29, 23.25, 14.41, 14.36, 14.22; ^{31}P NMR (121 MHz, CD_2Cl_2) δ 4.00 ($J_{P\text{-}Pt}$ = 2354 Hz); IR (KBr) ν 2056, 2098 cm^{-1}; HRMS (ESI-FTICR-MS) cald [M + H]; 2605.6877; found [M + H] 2605.6976: Anal. cald. for $C_{152}H_{236}N_2P_4Pt_2$ (%): C, 70.07; H, 9.13; N, 1.08; found C, 70.06; H, 9.43; N, 1.02.

4. X-Ray Diffraction Methods and Results for Compounds 1 and 2

A yellow crystal of **1** having approximate dimensions 0.22 mm x 0.23 mm x 0.53 mm was used for the X-ray crystallographic analysis. The X-ray intensity data were measured at 150 K on an Oxford Diffraction Xcalibur3 system equipped with a graphite monochromator and an Enhance (Mo) X-ray source (λ=0.71073 Å) operated at 2 kW power (50 kV and 40 mA). The detector was placed at a distance of 50 mm from the crystal. Final cell constants were obtained through a global refinement of all reflections. Intensity data were collected employing the *CrysAlis CCD* software program[5]. A series of 40-s data frames using φ and ω scans were integrated with the *CrysAlis RED*. The ω scan width was 1.0°. The integration of the data yielded a total of 89880 reflections to a maximum θ angle of 28.3° (0.75 Å resolution). The structure(Figure 1) was solved and refined using Bruker SHELXTL (v6.10). Crystal data: $C_{76}H_{94}N_2S_2P_2Pt$, MW =1356.68, Z = 2, monoclinic $P2_1/c$, a = 12.3121(4), b=12.4970(4), c = 22.8833(7) Å, α = 90°, β = 97.214(2)°, γ = 90°, V = 3493.05(19) Å^3, ρ_{calc} = 1.290 g cm^{-3}, 8536 unique reflections, 8427 with I > 2σ(I), μ = 2.156 mm^{-1}, anisotropic, hydrogen atoms isotropic, R = 0.0390 all reflections, R = 0.0383 > 2σ(I), wR = 0.0720 all reflections, wR = 0.0717 > 2σ(I), residual electron density minimum -0.681, residual electron density maximum 2.552 Å^{-3}.

X-ray intensity data from a yellow prism of **2** having approximate dimensions 0.073 mm x 0.11 mm x 0.32 mm were measured at 100 K. The detector was placed at a distance of 68.7 mm from the crystal. Final cell constants were obtained through a global

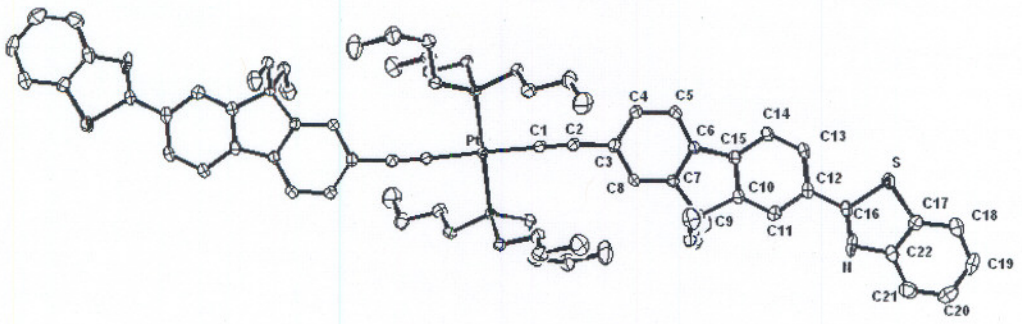

Figure 1. Molecular structure of **1**, with hydrogen atoms omitted for clarity and 50% probability displacement ellipsoids. Selected bond lengths(Å) and angles(deg): Pt-C1 = 2.000(3), C1-C2 = 1.208(4), C2-C3 = 1.442(4), C3-C4 = 1.406(4), C4-C5 = 1.391(4), C5-C6 = 1.395(4), C6–C7 = 1.401(4), C7–C9 = 1.525(4), C9-C10 = 1.525(4), C10-C11 = 1.374(4), C11–C12 = 1.411(4), C12–C13 = 1.399(4), C13-C14 = 1.387(4), C14-C15= 1.396(4), C12-C16 = 1.472(4), C16-N = 1.316(5), C16-S = 1.775(3), S-C17 = 1.734(3), C17-C18 = 1.395(5), C17-C22 = 1.396(4), C18-C19 = 1.393(6), C19-C20 = 1.393(6), C20-C21 = 1.367(5), C21-C22 = 1.383(5), Pt-C1-C2 = 176.6(3), C1-C2-C3 = 174.4(3), C3-C4-C5 = 121.1(3), C5-C6-C7 = 120.4(3), C6-C7-C9 = 111.1(2), C7-C9-C10 = 101.0(2), C9-C10-C11 = 128.4(3), C9-C10-C15= 110.9(3), C11-C12-C13 = 119.6(3), C13-C14-C15 = 118.7(3), C11-C12-C16 = 119.0(3), C13-C12-C16 = 121.3(3), N-C16-S = 116.5(2), S-C17-C22 = 110.9(2), S-C17-C18 = 127.8(3), C17-C18-C19 = 117.4(3), C19-C20-C21 = 121.3(4), C20-C21-C22 = 119.0(3), C21-C22-C17 = 120.2(3).

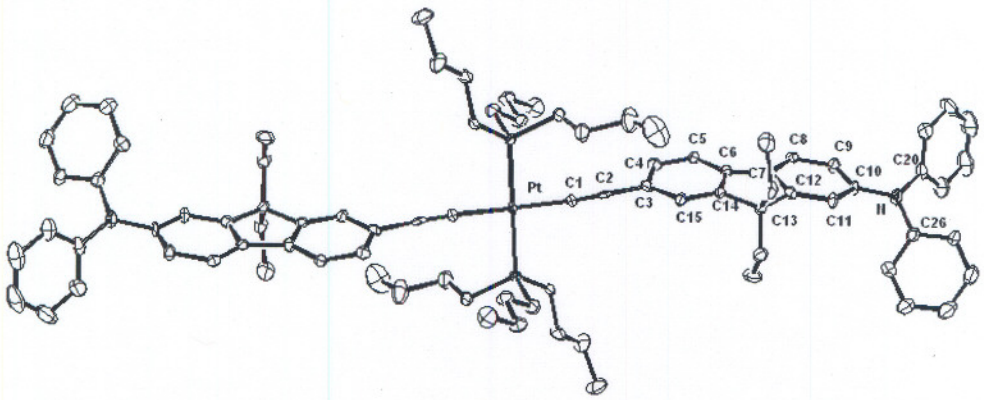

Figure 2. Molecular structure of **2**, with hydrogen atoms omitted for clarity and 50% probability displacement ellipsoids. Selected bond lengths(Å) and angles(deg): Pt-C1 = 2.023(8), C1-C2 = 1.144(12), C2-C3 = 1.487(11), C3-C4 = 1.404(12), C3-C15 = 1.407(11), C4-C5 = 1.403(11), C5-C6 = 1.393(10), C6-C7 = 1.475(10), C7-C8 = 1.390(11), C8-C9 = 1.411(11), C9-C10 = 1.411(12), C10-C11 = 1.394(11), C11-C12 = 1.395(10), C12-C13 = 1.529(11), C13-C14 = 1.512(10), C14-C15 = 1.370(11), C10-N = 1.419(9), N-C20 = 1.442(11), N-C26 = 1.419(12), Pt-C1-C2 = 176.8(8), C1-C2-C3 = 176.5(8), C3-C4-C5 = 121.3(8), C4-C5-C6 = 118.5(7), C5-C6-C7 = 131.2(7), C6-C7-C8 = 132.0(7), C7-C8-C9 = 119.2(7), C8-C9-C10 = 120.5(7), C9-C10-C11 = 119.5(7), C10-C11-C12 = 119.6(8), C11-C12-C13 = 127.5(7), C12-C13-C14 = 100.9(6), C10-N-C20 = 119.1(7), C10-N-C26 = 121.2(7), C20-N-C26 = 118.7(7).